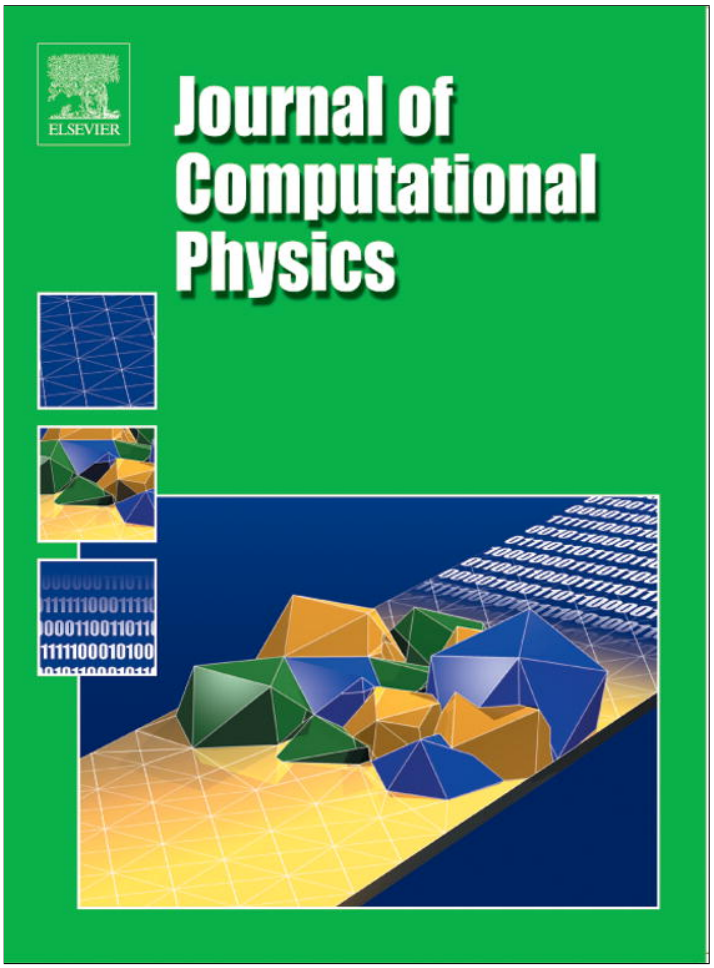

Journal of Computational Physics 242 (2013) 843–868

Contents lists available at SciVerse ScienceDirect

Journal of Computational Physics

journal homepage: www.elsevier.com/locate/jcp

A dynamically bi-orthogonal method for time-dependent stochastic partial differential equations I: Derivation and algorithms

Mulin Cheng, Thomas Y. Hou *, Zhiwen Zhang

Computing and Mathematical Sciences, California Institute of Technology, Pasadena, CA 91125, United States

ARTICLE INFO

Article history:
Available online 7 March 2013

Keywords:
Stochastic partial differential equations
Karhunen–Loeve expansion
Uncertainty quantification
Bi-orthogonality
Reduced-order model

ABSTRACT

We propose a dynamically bi-orthogonal method (DyBO) to solve time dependent stochastic partial differential equations (SPDEs). The objective of our method is to exploit some intrinsic sparse structure in the stochastic solution by constructing the sparsest representation of the stochastic solution via a bi-orthogonal basis. It is well-known that the Karhunen–Loeve expansion (KLE) minimizes the total mean squared error and gives the sparsest representation of stochastic solutions. However, the computation of the KL expansion could be quite expensive since we need to form a covariance matrix and solve a large-scale eigenvalue problem. The main contribution of this paper is that we derive an equivalent system that governs the evolution of the spatial and stochastic basis in the KL expansion. Unlike other reduced model methods, our method constructs the reduced basis on-the-fly without the need to form the covariance matrix or to compute its eigendecomposition. In the first part of our paper, we introduce the derivation of the dynamically bi-orthogonal formulation for SPDEs, discuss several theoretical issues, such as the dynamic bi-orthogonality preservation and some preliminary error analysis of the DyBO method. We also give some numerical implementation details of the DyBO methods, including the representation of stochastic basis and techniques to deal with eigenvalue crossing. In the second part of our paper [11], we will present an adaptive strategy to dynamically remove or add modes, perform a detailed complexity analysis, and discuss various generalizations of this approach. An extensive range of numerical experiments will be provided in both parts to demonstrate the effectiveness of the DyBO method.

1. Introduction

Uncertainty arises in many complex real-world problems of physical and engineering interests, such as wave, heat and pollution propagation through random media [30,19,17,52] and flow driven by stochastic forces [25,27,49,41,36]. Additional examples can be found in other branches of science and engineering, such as geosciences, statistical mechanics, meteorology, biology, finance, and social science. Stochastic partial differential equations (SPDEs) have played an important role in our investigation of uncertainty quantification (UQ). However, it is very challenging to solve stochastic PDEs efficiently due to the large dimensionality of stochastic solutions. Although many numerical methods have been proposed in the literature (see e.g. [51,9,12,13,23,29,37,53,4,5,54,35,50,27,47,1,38,24,45,14,33,15,16,39,43]), it is still very expensive to solve a time dependent nonlinear stochastic PDEs with high dimensional stochastic input variables. This limits our ability to attack some challenging real-world applications.

* Corresponding author.
E-mail addresses: mulinch@caltech.edu (M. Cheng), hou@cms.caltech.edu (T.Y. Hou), zhangzw@caltech.edu (Z. Zhang).

0021-9991/$ - see front matter © 2013 Elsevier Inc. All rights reserved.
http://dx.doi.org/10.1016/j.jcp.2013.02.033

In this paper, we propose a dynamically bi-orthogonal method (DyBO) to solve time-dependent stochastic partial differential equations. The dynamic bi-orthogonality condition that we impose on DyBO is closely related to the Karhunen–Loeve expansion (KLE) [28,31]. The KL expansion has received increasing attention in many fields, such as statistics, image processing, and uncertainty quantification. It yields the best basis in the sense that it minimizes the total mean squared error and gives the sparsest representation of stochastic solutions. However, computing KLE could be quite expensive since it involves forming a covariance matrix and solving the associated large-scale eigenvalue problem. One of the attractive features of our DyBO method is that we construct the sparsest bi-orthogonal basis on-the-fly without the need to form the covariance matrix or to compute its eigendecomposition.

We consider the following time-dependent stochastic partial differential equations:

$$\frac{\partial u}{\partial t}(x,t,\omega) = \mathcal{L}u(x,t,\omega), \quad x \in \mathcal{D} \subset \mathbb{R}^d, \quad \omega \in \Omega, \ t \in [0,T], \tag{1a}$$

$$u(x,0,\omega) = u_0(x,\omega), \quad x \in \mathcal{D}, \quad \omega \in \Omega, \tag{1b}$$

$$\mathcal{B}(u(x,t,\omega)) = h(x,t,\omega), \quad x \in \partial\mathcal{D}, \quad \omega \in \Omega, \tag{1c}$$

where $\mathcal{L}$ is a differential operator and may contain random coefficients and/or stochastic forces and $\mathcal{B}$ is a boundary operator. The randomness may also enter the system through the initial condition u_0 and/or the boundary conditions $\mathcal{B}$.

We assume the stochastic solution $u(x,t,\omega)$ of the system (1) is a second-order stochastic process, i.e., $u(\cdot,t,\cdot) \in \mathbb{L}^2(\mathcal{D}\times\Omega)$. The solution $u(x,t,\omega)$ can be represented by its KL expansion as follows:

$$u(x,t,\omega) = \bar{u}(x,t) + \sum_{i=1}^{\infty} u_i(x,t) Y_i(\omega,t), \tag{2}$$

where $\bar{u}(x,t) = \mathbb{E}[u(x,t,\omega)]$, u_i's are the eigenfunctions of the associated covariance function $\mathrm{Cov}_u(x,y) = \mathbb{E}[(u(x,t,\omega) - \bar{u}(x,t))(u(y,t,\omega) - \bar{u}(y,t))]$. Thus u_i are orthogonal to each other, i.e., $\langle u_i, u_j\rangle = \lambda_i\delta_{ij}$, where λ_i are the corresponding eigenvalues of the covariance function. The random variables Y_i have zero-mean and are mutually orthogonal, i.e. $\mathbb{E}[Y_iY_j] = \delta_{ij}$. They are defined as follows:

$$Y_i(\omega,t) = \frac{1}{\lambda_i(t)} \int_{\mathcal{D}} (u(x,t,\omega) - \bar{u}(x,t)) u_i(x,t)\,dx, \quad \text{for } i = 1,2,3,\ldots.$$

For many physical and engineering problems, the dimension of the input stochastic variables may appear to be high, but the effective dimension of the stochastic solution may be low due to the rapid decay of the eigenvalues λ_i [47]. For this type of problems, the KLE provides the sparest representation of the solution through an optimal set of bi-orthogonal spatial and stochastic basis. Since this bi-orthogonal basis is constructed at each time, both the spatial basis u_i and the stochastic basis Y_i are time-dependent to preserve bi-orthogonality. This is very different from other reduced-order basis in which either the spatial or the random basis is time-dependent, but not both of them are time-dependent. The traditional way to construct the KL expansion is to first solve SPDE by some conventional method, and then form the covariance function to construct the KL expansion. As we mentioned earlier, this post-processing approach is very expensive which would offset the benefit of giving a sparsest representation of the stochastic solution.

The main objective of this paper is to derive a well-posed system that governs the dynamic evolution of the KL expansion without the need of forming the covariance function explicitly. To illustrate the main idea, we assume that the eigenvalues λ_i decay rapidly and an m-term truncation in the KL expansion would give an accurate approximation of the stochastic solution. We substitute the m-term truncated expansion (2), denoted as $\tilde{u}$, into the stochastic PDE (1a). After projecting the resulting equation into the spatial and stochastic basis and using the bi-orthogonality of the basis, we obtain

$$\frac{\partial \bar{u}}{\partial t} = \mathbb{E}[\mathcal{L}\tilde{u}], \tag{3a}$$

$$\frac{\partial \mathbf{U}}{\partial t} = \mathbf{U}\boldsymbol{\Lambda}_{\mathbf{U}}^{-1}\left\langle \mathbf{U}^T, \frac{\partial \mathbf{U}}{\partial t}\right\rangle + G_{\mathbf{U}}(\bar{u},\mathbf{U},\mathbf{Y}), \tag{3b}$$

$$\frac{\mathrm{d}\mathbf{Y}}{\mathrm{d}t} = \mathbf{Y}\mathbb{E}\left[\mathbf{Y}^T\frac{\mathrm{d}\mathbf{Y}}{\mathrm{d}t}\right] + G_{\mathbf{Y}}(\bar{u},\mathbf{U},\mathbf{Y}), \tag{3c}$$

where $\mathbb{E}[\cdot]$ is the expectation, $\langle f, g\rangle = \int f(x)g(x)dx$, $\mathbf{U}(x,t) = (u_1(x,t), u_2(x,t), \ldots, u_m(x,t))$, $\mathbf{Y}(\omega,t) = (Y_1(\omega,t), Y_2(\omega,t), \ldots, Y_m(\omega,t))$, $\tilde{u} = \bar{u} + \mathbf{U}\mathbf{Y}^T$, $\boldsymbol{\Lambda}_{\mathbf{U}} = \mathrm{diag}(\left\langle \mathbf{U}^T, \mathbf{U}\right\rangle)$, $G_{\mathbf{U}}(\bar{u},\mathbf{U},\mathbf{Y})$ and $G_{\mathbf{Y}}(\bar{u},\mathbf{U},\mathbf{Y})$ are defined in (11a) and (11b) respectively. The initial condition of (3) is given by the KL expansion of $u_0(x,\omega)$.

A close inspection shows that the evolution system (3b) and (3c) does not determine the time derivative $\frac{\partial \mathbf{U}}{\partial t}$ or $\frac{\mathrm{d}\mathbf{Y}}{\mathrm{d}t}$ uniquely. In fact, (3b) only determines the projection of $\frac{\partial \mathbf{U}}{\partial t}$ into the orthogonal complement set of $\mathbf{U}$ uniquely, which is $G_{\mathbf{U}}$. Similarly, (3c) only determines the projection of $\frac{\mathrm{d}\mathbf{Y}}{\mathrm{d}t}$ into the orthogonal complement set of $\mathbf{Y}$ uniquely, which is $G_{\mathbf{Y}}$. Thus, the evolution system (3) can be rewritten as follows:

$$\frac{\partial \bar{u}}{\partial t} = \mathbb{E}[\mathcal{L}\tilde{u}], \tag{4a}$$

$$\frac{\partial \mathbf{U}}{\partial t} = \mathbf{UC} + G_{\mathbf{U}}(\bar{u}, \mathbf{U}, \mathbf{Y}), \tag{4b}$$

$$\frac{\mathrm{d}\mathbf{Y}}{\mathrm{d}t} = \mathbf{YD} + G_{\mathbf{Y}}(\bar{u}, \mathbf{U}, \mathbf{Y}), \tag{4c}$$

where $\mathbf{C}$ and $\mathbf{D}$ are $m \times m$ matrices which represent the projection coefficients of $\frac{\partial \mathbf{U}}{\partial t}$ and $\frac{\mathrm{d}\mathbf{Y}}{\mathrm{d}t}$ into $\mathbf{U}$ and $\mathbf{Y}$ respectively. These two matrices characterize the large degrees of freedom in choosing the spatial and stochastic basis dynamically. They cannot be chosen independently. Instead, they must satisfy a compatibility condition to be consistent with the original SPDE and satisfy the bi-orthogonality condition of the spatial and the stochastic basis. By introducing two types of antisymmetric operators to enforce the bi-orthogonality condition, we derive two constraints for C and D. When combining these two constraints with the compatibility condition, we show that these two matrices can be determined uniquely provided that the eigenvalues of the covariance matrix are distinct.

We prove rigorously that the system of governing equations indeed preserve the bi-orthogonality condition dynamically. More precisely, if we write $\boldsymbol{\chi}(t) = (\langle u_i, u_j \rangle_{i>j})$ as a column vector in $\mathbb{R}^{\frac{m(m-1)}{2}\times 1}$, then $\boldsymbol{\chi}(t)$ satisfies a linear ODE system $\frac{\mathrm{d}\boldsymbol{\chi}(t)}{\mathrm{d}t} = \mathcal{W}(t)\boldsymbol{\chi}(t)$ for some anti-symmetric matrix $\mathcal{W}(t)$. The fact that $\mathcal{W}(t)$ is anti-symmetric is important because this implies that the dynamic preservation of bi-orthogonality condition is very stable to perturbation and any deviation from the bi-orthogonal form will not be amplified.

The breakdown in deriving a well-posed system for the KL expansion when two distinct eigenvalues coincide dynamically is associated with additional degrees of freedom in choosing orthogonal eigenvectors. To overcome this difficulty, we design a strategy to handle eigenvalue crossings. When two distinct eigenvalues become close, we temporarily freeze the stochastic basis and evolve only the spatial basis. By doing so, we still maintain the dynamic orthogonality of the stochastic basis, which allows us to compute the covariance matrix relatively easily. After the two eigenvalues separate in time, we can reinitialize the DyBO method by reconstructing the KL expansion without forming the covariance matrix. Similarly, we can freeze the spatial basis and evolve the stochastic basis for a short time until the two eigenvalues are separated.

We remark that the low-dimensional or sparse structures of SPDE solutions have been explored *partially* in some methods, such as the proper orthogonal decomposition (POD) methods [3,48,49], reduced-basis (RB) methods [7,34,44,21], and dynamical orthogonal method (DO) [45,46]. Our method shares some common feature with the dynamically orthogonal method since both methods use time-dependent spatial and stochastic basis. An important ingredient in POD and RB methods is how to choose the reduced basis from some limited information of the solution that we learn offline. The main difference between our method and other reduced basis methods is that we bypass the step of learning the basis offline, which in general can be quite expensive. We construct the reduced basis on the fly as we solve the SPDE.

We have performed some preliminary error analysis for our method. In the case when the differential operator is linear and deterministic and the randomness enters through the initial condition or forcing, we show that the error is due to the projection of the initial condition or the random forcing into the bi-orthogonal basis. In the special case when the initial condition has exactly m modes in the KL expansion, the m-term DyBO method will reproduce the exact solution without any error. For general nonlinear stochastic PDEs, the number of effective modes in the KL expansion will increase dynamically due to nonlinear interaction. In this case, even if the initial condition has an exactly m-mode KL expansion, we must dynamically increase modes to maintain the accuracy of our computation.

We have developed an effective adaptive strategy for DyBO to add or remove modes dynamically to maintain a desirable accuracy. If the magnitude of the last mode falls below a prescribed tolerance, we can remove this mode dynamically. On the other hand, when the magnitude of the last mode rises above a certain tolerance, we need to add a new mode pair. The method we propose to add new modes dynamically is to use the DyBO solution as the initial condition and compute a DyBO solution and a generalized Polynomial Chaos (gPC) solution respectively for a short time. We then compute the KL expansion of the difference between the DyBO solution and the gPC solution. We add the largest mode from the KL expansion of the difference to our DyBO method. This method works quite effectively. More details will be reported in the second part of our paper [11].

As we will demonstrate in our paper, the DyBO method could offer accurate numerical solutions to SPDEs with significant computational saving over traditional stochastic methods. We have performed numerical experiments for 1D Burgers equations, 2D incompressible Navier–Stokes equations, and Boussinesq equations with approximated Brownian motion forcing. In all these cases, we observe considerable computational saving. The specific rate of saving will depend on how we discretize the stochastic ordinary differential equations (SODEs) governing the stochastic basis. We can use three methods to discretize the SODEs, i.e. (i) Monte Carlo methods (MC), (ii) generalized stochastic collocation methods (gSC), (iii) generalized polynomial chaos methods (gPC). In the numerical experiments we present in this paper, we use gPC to discretize the SODE. Our numerical results show that the DyBO method gives much faster decay rate for its error compared with that of the gPC method. To illustrate this point, we show the sorted energy spectrum of the solution of the stochastically forced Burgers equation computed by our DyBO method and that of the gPC method respectively in Fig. 1. We can see that the eigenvalues of the covariance matrix decay much faster than the corresponding sorted energy spectrum of the gPC solution, indicating the effective dimension reduction induced by the bi-orthogonal basis. If we denote m as the number of modes used by DyBO

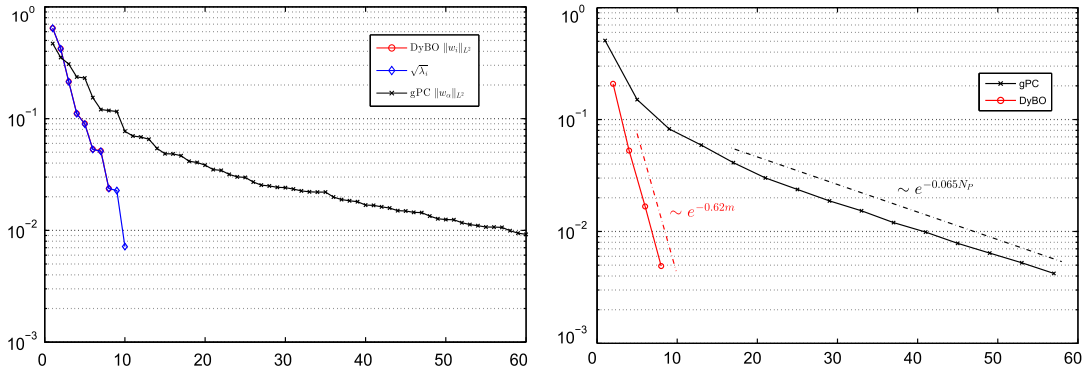

Fig. 1. Stochastically forced Burgers equations computed by DyBO and gPC. Left: (Sorted) Energy spectrum of gPC and DyBO solutions. Right: Relative errors of STD, DyBO ($e^{-0.62m}$) vs gPC ($e^{-0.065N_p}$).

and N_p the number of modes used by gPC, our complexity analysis shows that the ratio between the computational complexities of DyBO and gPC is roughly of order $O(m/N_p)^3$ for a two-dimensional quadratic nonlinear SPDE. Typically m is much smaller than N_p, as illustrated in Fig. 1. More details can be found in part II of our paper where we also discuss the parallel implementation of DyBO [11].

This paper is organized as follows. In Section 2, we provide the detailed derivation of the DyBO formulation for a time-dependent SPDE. Some important theoretic aspects of the DyBO formulation, such as bi-orthogonality preservation and the consistency between the DyBO formulation and the original SPDE are discussed in Section 3. In Section 4, we discuss some detailed numerical implementations of the DyBO method, such as the representation of the stochastic basis $\mathbf{Y}$ and a strategy to deal with eigenvalue crossings. Three numerical examples are provided in Section 5 to demonstrate computational advantage of our DyBO method. Finally, some remarks will be made in Section 6.

2. Derivation of dynamically bi-orthogonal formulation

In this section, we introduce the derivation of our dynamically bi-orthogonal method. For the ease of future derivations, we use extensively vector and matrix notations.

$$\mathbf{U}(x,t) = (u_1(x,t), u_2(x,t), \ldots, u_m(x,t)), \quad \tilde{\mathbf{U}}(x,t) = (u_{m+1}(x,t), u_{m+2}(x,t), \ldots),$$
$$\mathbf{Y}(\omega,t) = (Y_1(\omega,t), Y_2(\omega,t), \ldots, Y_m(\omega,t)), \quad \tilde{\mathbf{Y}}(\omega,t) = (Y_{m+1}(\omega,t), Y_{m+2}(\omega,t), \ldots).$$

Correspondingly, $\mathbb{E}[\mathbf{Y}^T\mathbf{Y}]$ and $\left\langle \mathbf{U}^T, \mathbf{U} \right\rangle$ are m-by-m matrices and the bi-orthogonality condition can be rewritten compactly as

$$\mathbb{E}\left[\mathbf{Y}^T\mathbf{Y}\right](t) = \left(\mathbb{E}\left[Y_i Y_j\right]\right) = \mathbf{I} \in \mathbb{R}^{m\times m}, \tag{5a}$$

$$\left\langle \mathbf{U}^T, \mathbf{U} \right\rangle(t) = \left(\left\langle u_i, u_j \right\rangle\right) = \mathbf{\Lambda}_{\mathbf{U}} \in \mathbb{R}^{m\times m}, \tag{5b}$$

where $\mathbf{\Lambda}_{\mathbf{U}} = \mathrm{diag}\left(\left\langle \mathbf{U}^T, \mathbf{U} \right\rangle\right) = (\lambda_i \delta_{ij})_{m\times m}$. Therefore, the KL expansion (2) of u at some fixed time t reads

$$u = \bar{u} + \mathbf{U}\mathbf{Y}^T + \tilde{\mathbf{U}}\tilde{\mathbf{Y}}^T. \tag{6}$$

Furthermore, we assume that the solution of the SPDE (1) enjoys a low-dimensional structure in the sense of KLE, or precisely, the eigenvalue spectrum $\{\lambda_i(t)\}_{i=1}^{\infty}$ decays fast enough, allowing for a good approximation with a truncated KL expansion (2). We denote by $\tilde{u}$ as the m-term truncation of the KL expansion of u,

$$\tilde{u} = \bar{u} + \mathbf{U}\mathbf{Y}^T. \tag{7}$$

We introduce the following orthogonal complementary operators with respect to the orthogonal basis $\mathbf{U}$ in $\mathbb{L}^2(\mathcal{D})$ or $\mathbf{Y}$ in $\mathbb{L}^2(\Omega)$ to simplify notations,

$$\Pi_{\mathbf{U}}(v) = v - \mathbf{U}\mathbf{\Lambda}_{\mathbf{U}}^{-1}\left\langle \mathbf{U}^T, v \right\rangle \quad \text{for } v(x) \in \mathbb{L}^2(\mathcal{D}),$$
$$\Pi_{\mathbf{Y}}(Z) = Z - \mathbf{Y}\mathbb{E}\left[\mathbf{Y}^T Z\right] \quad \text{for } Z(\omega) \in \mathbb{L}^2(\Omega).$$

We also define an anti-symmetrization operator $\mathcal{Q} : \mathbb{R}^{k\times k} \to \mathbb{R}^{k\times k}$ and a partial anti-symmetrization operator $\tilde{\mathcal{Q}} : \mathbb{R}^{k\times k} \to \mathbb{R}^{k\times k}$, which are defined as follows:

$$\mathcal{Q}(\mathbf{A}) = \frac{1}{2}\left(\mathbf{A} - \mathbf{A}^T\right), \quad \tilde{\mathcal{Q}}(\mathbf{A}) = \frac{1}{2}\left(\mathbf{A} - \mathbf{A}^T\right) + \mathrm{diag}(\mathbf{A}),$$

where diag($\mathbf{A}$) denotes a diagonal matrix whose diagonal entries are equal to those of matrix $\mathbf{A}$.

In the DyBO formulation it is crucial to dynamically preserve the bi-orthogonality of the spatial basis $\mathbf{U}$ and the stochastic basis $\mathbf{Y}$. We begin the derivation by substituting the KLE (2) into the SPDE (1a) and get

$$\frac{\partial \bar{u}}{\partial t}+\frac{\partial \mathbf{U}}{\partial t}\mathbf{Y}^T+\mathbf{U}\frac{\mathrm{d}\mathbf{Y}^T}{\mathrm{d}t}=\mathcal{L}\tilde{u}+\{\mathcal{L}u-\mathcal{L}\tilde{u}\}-\left\{\frac{\partial \tilde{\mathbf{U}}}{\partial t}\tilde{\mathbf{Y}}^T+\tilde{\mathbf{U}}\frac{\mathrm{d}\tilde{\mathbf{Y}}^T}{\mathrm{d}t}\right\}.$$

If the eigenvalues in the KL expansion decay fast enough and the differential operator is stable, the last two terms on the right hand side will be small, so we can drop them and obtain the starting point for deriving our DyBO method,

$$\frac{\partial \bar{u}}{\partial t}+\frac{\partial \mathbf{U}}{\partial t}\mathbf{Y}^T+\mathbf{U}\frac{\mathrm{d}\mathbf{Y}^T}{\mathrm{d}t}=\mathcal{L}\tilde{u}. \tag{8}$$

Taking expectations on both sides of Eq. (8) and taking into account the fact that Y_i's are zero-mean random variables, we have

$$\frac{\partial \bar{u}}{\partial t}=\mathbb{E}[\mathcal{L}\tilde{u}],$$

which gives the evolution equation for the mean of the solution u. Multiplying both sides of Eq. (8) by $\mathbf{Y}$ from the right and taking expectations, we obtain

$$\frac{\partial \mathbf{U}}{\partial t}\mathbb{E}\left[\mathbf{Y}^T\mathbf{Y}\right]+\mathbf{U}\mathbb{E}\left[\frac{\mathrm{d}\mathbf{Y}^T}{\mathrm{d}t}\mathbf{Y}\right]=\mathbb{E}\left[(\mathcal{L}\tilde{u}-\frac{\partial \bar{u}}{\partial t})\mathbf{Y}\right].$$

After using the orthogonality of the stochastic basis $\mathbf{Y}$, we have

$$\frac{\partial \mathbf{U}}{\partial t}=\mathbb{E}\left[\tilde{\mathcal{L}}\tilde{u}\mathbf{Y}\right]-\mathbf{U}\mathbb{E}\left[\frac{\mathrm{d}\mathbf{Y}^T}{\mathrm{d}t}\mathbf{Y}\right],$$

where $\tilde{\mathcal{L}}\tilde{u}=\mathcal{L}\tilde{u}-\mathbb{E}[\mathcal{L}\tilde{u}]$. Similarly we obtain an evolution equation for $\frac{\mathrm{d}\mathbf{Y}}{\mathrm{d}t}$. Therefore, this gives rise to the following evolution system:

$$\frac{\partial \bar{u}}{\partial t}=\mathbb{E}[\mathcal{L}\tilde{u}], \tag{9a}$$

$$\frac{\partial \mathbf{U}}{\partial t}=\mathbb{E}\left[\tilde{\mathcal{L}}\tilde{u}\mathbf{Y}\right]-\mathbf{U}\mathbb{E}\left[\frac{\mathrm{d}\mathbf{Y}^T}{\mathrm{d}t}\mathbf{Y}\right], \tag{9b}$$

$$\frac{\mathrm{d}\mathbf{Y}}{\mathrm{d}t}\mathbf{\Lambda}_{\mathbf{U}}=\langle\tilde{\mathcal{L}}\tilde{u},\mathbf{U}\rangle-\mathbf{Y}\left\langle\frac{\partial \mathbf{U}^T}{\partial t},\mathbf{U}\right\rangle. \tag{9c}$$

However, the above system does not give explicit evolution equations for $\frac{\mathrm{d}\mathbf{Y}}{\mathrm{d}t}$ and $\frac{\partial \mathbf{U}}{\partial t}$. To further simplify the evolution system, we substitute Eq. (9c) into Eq. (9b) and get

$$\frac{\partial \mathbf{U}}{\partial t}=\mathbb{E}\left[\tilde{\mathcal{L}}\tilde{u}\mathbf{Y}\right]-\mathbf{U}\mathbf{\Lambda}_{\mathbf{U}}^{-1}\left\langle\mathbf{U}^T,\mathbb{E}\left[\tilde{\mathcal{L}}\tilde{u}\mathbf{Y}\right]\right\rangle+\mathbf{U}\mathbf{\Lambda}_{\mathbf{U}}^{-1}\left\langle\mathbf{U}^T,\frac{\partial \mathbf{U}}{\partial t}\right\rangle,$$

where we have used the orthogonality of the stochastic basis, i.e., $\mathbb{E}\left[\mathbf{Y}^T\mathbf{Y}\right]=\mathbf{I}$. Similar steps can be repeated by substituting Eq. (9b) into Eq. (9c). Thus, the system (9) can be re-written as

$$\frac{\partial \bar{u}}{\partial t}=\mathbb{E}[\mathcal{L}\tilde{u}], \tag{10a}$$

$$\frac{\partial \mathbf{U}}{\partial t}=\mathbf{U}\mathbf{\Lambda}_{\mathbf{U}}^{-1}\left\langle\mathbf{U}^T,\frac{\partial \mathbf{U}}{\partial t}\right\rangle+G_{\mathbf{U}}(\bar{u},\mathbf{U},\mathbf{Y}), \tag{10b}$$

$$\frac{\mathrm{d}\mathbf{Y}}{\mathrm{d}t}=\mathbf{Y}\mathbb{E}\left[\mathbf{Y}^T\frac{\mathrm{d}\mathbf{Y}}{\mathrm{d}t}\right]+G_{\mathbf{Y}}(\bar{u},\mathbf{U},\mathbf{Y}), \tag{10c}$$

where we have used the orthogonality condition of the spatial and stochastic modes, and

$$G_{\mathbf{U}}(\bar{u},\mathbf{U},\mathbf{Y})=\Pi_{\mathbf{U}}(\mathbb{E}\left[\tilde{\mathcal{L}}\tilde{u}\mathbf{Y}\right])=\mathbb{E}\left[\tilde{\mathcal{L}}\tilde{u}\mathbf{Y}\right]-\mathbf{U}\mathbf{\Lambda}_{\mathbf{U}}^{-1}\left\langle\mathbf{U}^T,\mathbb{E}\left[\tilde{\mathcal{L}}\tilde{u}\mathbf{Y}\right]\right\rangle, \tag{11a}$$

$$G_{\mathbf{Y}}(\bar{u},\mathbf{U},\mathbf{Y})=\Pi_{\mathbf{Y}}(\langle\tilde{\mathcal{L}}\tilde{u},\mathbf{U}\rangle)\mathbf{\Lambda}_{\mathbf{U}}^{-1}=\langle\tilde{\mathcal{L}}\tilde{u},\mathbf{U}\rangle\mathbf{\Lambda}_{\mathbf{U}}^{-1}-\mathbf{Y}\left\langle\mathbb{E}\left[\tilde{\mathcal{L}}\tilde{u}\mathbf{Y}^T\right],\mathbf{U}\right\rangle\mathbf{\Lambda}_{\mathbf{U}}^{-1}. \tag{11b}$$

Note that $G_{\mathbf{U}}$ is the projection of $\mathbb{E}[\tilde{\mathcal{L}}\tilde{u}\mathbf{Y}]$ into the orthogonal complementary set of $\mathbf{U}$ and $G_{\mathbf{Y}}$ is the projection of $\langle\tilde{\mathcal{L}}\tilde{u},\mathbf{U}\rangle$ into the orthogonal complementary set of $\mathbf{Y}$. Thus, we have

$$G_{\mathbf{U}}(\bar{u},\mathbf{U},\mathbf{Y})\perp \text{span}\mathbf{U}\quad \text{in}\mathbb{L}^2(\mathcal{D}),\qquad G_{\mathbf{Y}}(\bar{u},\mathbf{U},\mathbf{Y})\perp \text{span}\mathbf{Y}\quad \text{in}\mathbb{L}^2(\Omega).$$

The above observation will be crucial in the later derivations.

We note that the system (10b) and (10c) does not determine the time derivative $\frac{\partial\mathbf{U}}{\partial t}$ or $\frac{\mathrm{d}\mathbf{Y}}{\mathrm{d}t}$ uniquely. In fact, if $\frac{\partial\mathbf{U}}{\partial t}$ is a solution of (10b), then $\frac{\partial\mathbf{U}}{\partial t}+\mathbf{UC}$ for any $m\times m$ matrix $\mathbf{C}$ is also a solution of (10b). Similar statement can be made for $\frac{\mathrm{d}\mathbf{Y}}{\mathrm{d}t}$. In Appendix A, we will show that the evolution system (3) can be rewritten as follows:

$$\frac{\partial\bar{u}}{\partial t}=\mathbb{E}[\mathcal{L}\tilde{u}], \tag{12a}$$

$$\frac{\partial\mathbf{U}}{\partial t}=\mathbf{UC}+G_{\mathbf{U}}(\bar{u},\mathbf{U},\mathbf{Y}), \tag{12b}$$

$$\frac{\mathrm{d}\mathbf{Y}}{\mathrm{d}t}=\mathbf{YD}+G_{\mathbf{Y}}(\bar{u},\mathbf{U},\mathbf{Y}), \tag{12c}$$

where $\mathbf{C}$ and $\mathbf{D}$ are $m\times m$ matrices which represent the projection coefficients of $\frac{\partial\mathbf{U}}{\partial t}$ and $\frac{\mathrm{d}\mathbf{Y}}{\mathrm{d}t}$ into $\mathbf{U}$ and $\mathbf{Y}$ respectively. Moreover, we show that by enforcing the bi-orthogonality condition of the spatial and stochastic basis and a compatibility condition with the original SPDE, these two matrices can be determined uniquely provided that the eigenvalues of the covariance matrix are distinct. The results are summarized in the following theorem.

Theorem 2.1 (*Solvability of matrices* $\mathbf{C}$ *and* $\mathbf{D}$). *If* $\langle u_i,u_i\rangle\neq\langle u_j,u_j\rangle$ *for* $i\neq j,i,j=1,2,\ldots,m$, *the* m*-by-*m *matrices* $\mathbf{C}$ *and* $\mathbf{D}$ *can be solved uniquely from the following linear system*

$$\mathbf{C}-\mathbf{\Lambda}_{\mathbf{U}}^{-1}\tilde{\mathcal{Q}}(\mathbf{\Lambda}_{\mathbf{U}}\mathbf{C})=0, \tag{13a}$$

$$\mathbf{D}-\mathcal{Q}(\mathbf{D})=0, \tag{13b}$$

$$\mathbf{D}^T+\mathbf{C}=G_*(\bar{u},\mathbf{U},\mathbf{Y}), \tag{13c}$$

where $G_*(\bar{u},\mathbf{U},\mathbf{Y})=\mathbf{\Lambda}_{\mathbf{U}}^{-1}\left\langle\mathbf{U}^T,\mathbb{E}[\tilde{\mathcal{L}}\tilde{u}\mathbf{Y}]\right\rangle\in\mathbb{R}^{m\times m}$. The solutions are given entry-wisely as follows:

$$C_{ii}=G_{*ii}, \tag{14a}$$

$$C_{ij}=\frac{\|u_j\|^2_{\mathbb{L}^2(\mathcal{D})}}{\|u_j\|^2_{\mathbb{L}^2(\mathcal{D})}-\|u_i\|^2_{\mathbb{L}^2(\mathcal{D})}}(G_{*ij}+G_{*ji}),\quad \text{for } i\neq j, \tag{14b}$$

$$D_{ii}=0, \tag{14c}$$

$$D_{ij}=\frac{1}{\|u_j\|^2_{\mathbb{L}^2(\mathcal{D})}-\|u_i\|^2_{\mathbb{L}^2(\mathcal{D})}}(\|u_j\|^2_{\mathbb{L}^2(\mathcal{D})}G_{*ji}+\|u_i\|^2_{\mathbb{L}^2(\mathcal{D})}G_{*ij}),\quad \text{for } i\neq j. \tag{14d}$$

To summarize the above discussion, the DyBO formulation of SPDE (1) results in a set of explicit equations for all the unknowns quantities. In particular, we reformulate the original SPDE (1) into a system of m stochastic ordinary differential equations for the stochastic basis $\mathbf{Y}$ coupled with $m+1$ deterministic PDEs for the mean solution $\bar{u}$ and spatial basis $\mathbf{U}$. Further, from the definition of G_* given in Theorem 2.1, we can rewrite $G_{\mathbf{U}}$ and $G_{\mathbf{Y}}$ as

$$G_{\mathbf{U}}=\mathbb{E}[\tilde{\mathcal{L}}\tilde{u}\mathbf{Y}]-\mathbf{U}G_*,\quad G_{\mathbf{Y}}=\langle\tilde{\mathcal{L}}\tilde{u},\mathbf{U}\rangle\mathbf{\Lambda}_{\mathbf{U}}^{-1}-\mathbf{Y}G_*^T.$$

From the above identities, we can rewrite the DyBO formulation (12) as follows:

$$\frac{\partial\bar{u}}{\partial t}=\mathbb{E}[\mathcal{L}\tilde{u}], \tag{15a}$$

$$\frac{\partial\mathbf{U}}{\partial t}=-\mathbf{UD}^T+\mathbb{E}[\tilde{\mathcal{L}}\tilde{u}\mathbf{Y}], \tag{15b}$$

$$\frac{\mathrm{d}\mathbf{Y}}{\mathrm{d}t}=-\mathbf{YC}^T+\langle\tilde{\mathcal{L}}\tilde{u},\mathbf{U}\rangle\mathbf{\Lambda}_{\mathbf{U}}^{-1}, \tag{15c}$$

where we have used the compatibility condition Eq. (13c) for C and D, i.e., $\mathbf{D}^T+\mathbf{C}=G_*$. The initial conditions of $\bar{u},\mathbf{U}$ and $\mathbf{Y}$ are given by the KL expansion of $u_0(x,\omega)$ in Eq. (1b). We can derive the boundary condition of $\bar{u}$ and the spatial basis $\mathbf{U}$ by taking expectation on the boundary condition. For example, if $\mathcal{B}$ is a linear deterministic differential operator, we have $\mathcal{B}(\bar{u}(x,t,\omega))|_{x\in\partial D}=\mathbb{E}[h(x,t,\omega)]$ and $\mathcal{B}(u_i(x,t,\omega))|_{x\in\partial D}=\mathbb{E}[h(x,t,\omega)Y_i(\omega,t)]$. If the periodic boundary condition is used in Eq. (1c), $\bar{u}$ and the spatial basis $\mathbf{U}$ satisfy the periodic boundary condition.

Remark 2.1. In the event that two eigenvalues approach each other and then separate as time increases, we refer to this as eigenvalue crossings. The breakdown in determining matrices **C** and **D** when we have eigenvalue crossings represents the extra degrees of freedom in choosing a complete set of orthogonal eigenvectors for repeated eigenvalues. To overcome this difficulty associated with eigenvalue crossings, we can detect such an event and temporarily *freeze* the spatial basis **U** or the stochastic basis **Y** and continue to evolve the system for a short duration. Once the two eigenvalues separate, the solution can be recast into the bi-orthogonal form via KL expansion. Recall that one of **U** and **Y** is always kept orthogonal even during the "freezing" stage. We can devise a KL expansion algorithm which avoids the need to form the covariance function explicitly. More details will be discussed in the section about numerical implementation.

3. Theoretical analysis

3.1. Bi-orthogonality preservation

In the previous section, we have used the bi-orthogonal condition in deriving our DyBO method. Since we have made a number of approximations by using a finite truncation of the KL expansion and performing various projections, these formal derivations do not necessarily guarantee that the DyBO method actually preserves the bi-orthogonal condition. In this section, we will show that the DyBO formulation (15) preserves the bi-orthogonality of the spatial basis **U** and the stochastic basis **Y** for $t \in [0, T]$ if the bi-orthogonality condition is satisfied initially.

Theorem 3.1 (*Preservation of Bi-Orthogonality in DyBO formulation*). *Assume that there is no eigenvalue crossing up to time* $T > 0$, *i.e.* $\|u_j\|_{\mathbb{L}^2(\mathcal{D})} \neq \|u_i\|_{\mathbb{L}^2(\mathcal{D})}$ *for* $i \neq j$. *The solutions* **U** *and* **Y** *of system* (15) *satisfy the bi-orthogonality condition* (5) *exactly as long as the initial conditions* $\mathbf{U}(x,0)$ *and* $\mathbf{Y}(\omega,0)$ *satisfy the bi-orthogonality condition* (5). *Moreover, if we write* $\chi_{(i,j)}(t) = \langle u_i, u_j\rangle(t)$ *for* $i > j$ *and denote* $\boldsymbol{\chi}(t) = (\chi_{(i,j)}(t))_{i>j}$ *as a column vector in* $\mathbb{R}^{\frac{m(m-1)}{2}\times 1}$, *then there exists an anti-symmetric matrix* $\mathcal{W}(t) \in \mathbb{R}^{\frac{m(m-1)}{2}\times\frac{m(m-1)}{2}}$ *such that*

$$\frac{\mathrm{d}\boldsymbol{\chi}(t)}{\mathrm{d}t} = \mathcal{W}(t)\boldsymbol{\chi}(t), \tag{16a}$$

$$\boldsymbol{\chi}(0) = 0. \tag{16b}$$

Similar results also hold for the stochastic basis **Y**.

Remark 3.1. The fact that $\mathcal{W}(t)$ is anti-symmetric is important for the stability of our DyBO method in preserving the dynamic bi-orthogonality of the spatial and stochastic basis. Due to numerical round-off errors, discretization errors, etc., **U** and **Y** may not be perfectly bi-orthogonal at the beginning or become so later in the computation. The above theorem sheds some lights on the numerical stability of DyBO formulation in this scenario. Since the eigenvalues of an anti-symmetric matrix are purely imaginary or zero and their geometric multiplicities are always one (see page 115, [22]), so any deviation from the bi-orthogonal form will not be amplified.

Proof. Proof of Theorem 3.1] We only give the proof for the spatial basis **U**, since the proof for the stochastic basis **Y** is similar. Direct computations give

$$\begin{aligned}\frac{\mathrm{d}}{\mathrm{d}t}\langle\mathbf{U}^T,\mathbf{U}\rangle &= \left\langle\frac{\partial\mathbf{U}^T}{\partial t},\mathbf{U}\right\rangle + \left\langle\mathbf{U}^T,\frac{\partial\mathbf{U}}{\partial t}\right\rangle = -\mathbf{D}\left\langle\mathbf{U}^T,\mathbf{U}\right\rangle + \left\langle\mathbb{E}\left[\tilde{\mathcal{L}}\tilde{u}\mathbf{Y}^T\right],\mathbf{U}\right\rangle - \left\langle\mathbf{U}^T,\mathbf{U}\right\rangle\mathbf{D}^T + \left\langle\mathbf{U}^T,\mathbb{E}\left[\tilde{\mathcal{L}}\tilde{u}\mathbf{Y}\right]\right\rangle\\ &= -\mathbf{D}\left\langle\mathbf{U}^T,\mathbf{U}\right\rangle - \left\langle\mathbf{U}^T,\mathbf{U}\right\rangle\mathbf{D}^T + G_*^T\boldsymbol{\Lambda}_{\mathbf{U}} + \boldsymbol{\Lambda}_{\mathbf{U}}G_*,\end{aligned} \tag{17}$$

where we have used the definition of G_* (see Theorem 2.1 and (A.13)) in the last equality. For each entry with $i \neq j$ in (17), we get,

$$\begin{aligned}\frac{\mathrm{d}}{\mathrm{d}t}\langle u_i,u_j\rangle &= -\sum_{k=1}^{m}D_{ik}\langle u_k,u_j\rangle - \sum_{l=1}^{m}\langle u_i,u_l\rangle D_{jl} + G_{*ji}\|u_j\|^2_{\mathbb{L}^2(\mathcal{D})} + G_{*ij}\|u_i\|^2_{\mathbb{L}^2(\mathcal{D})}\\ &= -\sum_{k=1,k\neq j}^{m}D_{ik}\langle u_k,u_j\rangle - \sum_{l=1,l\neq i}^{m}\langle u_i,u_l\rangle D_{jl} - D_{ij}\|u_j\|^2_{\mathbb{L}^2(\mathcal{D})} - D_{ji}\|u_i\|^2_{\mathbb{L}^2(\mathcal{D})} + (\|u_j\|^2_{\mathbb{L}^2(\mathcal{D})} - \|u_i\|^2_{\mathbb{L}^2(\mathcal{D})})D_{ij}\\ &= -\sum_{k=1,k\neq i,j}^{m}D_{ik}\langle u_k,u_j\rangle - \sum_{l=1,l\neq i,j}^{m}D_{jl}\langle u_i,u_l\rangle,\end{aligned} \tag{18}$$

where Eq. (14d) and the anti-symmetric property of matrix **D** are used. From Eq. (18), we see that $\boldsymbol{\chi}(t)$ satisfies a linear ODE system in the form of (16) with matrix $\mathcal{W}(t)$ given in terms of D_{ij} and the initial condition comes from the fact that $\mathbf{U}(x,0)$ are

a set of orthogonal basis. It is easy to see that, as long as the solutions of system (15) exist, $\mathcal{W}(t)$ is well-defined and the ODE system admits only zero solution, i.e., orthogonality of $\mathbf{U}$ is preserved for $t \in [0,T]$. Similar arguments can be used to show $\mathbf{Y}$ remains orthonormal for $t \in [0,T]$.

Next, we show that the matrix $\mathcal{W}$ in ODE system (16) is anti-symmetric. Consider two pairs of indices (i,j) and (p,q) with $i>j$ and $p>q$. The corresponding equations for $\chi_{(i,j)}$ and $\chi_{(p,q)}$ are

$$\frac{\mathrm{d}\chi_{(i,j)}}{\mathrm{d}t} = -\sum_{k=1,k\neq i,j}^{m} D_{ik}\chi_{(k,j)} - \sum_{l=1,l\neq i,j}^{m} D_{jl}\chi_{(i,l)}, \tag{19a}$$

$$\frac{\mathrm{d}\chi_{(p,q)}}{\mathrm{d}t} = -\sum_{k=1,k\neq p,q}^{m} D_{pk}\chi_{(k,q)} - \sum_{l=1,l\neq p,q}^{m} D_{ql}\chi_{(p,l)}, \tag{19b}$$

where we have identified $\chi_{(i,j)}$ with $\chi_{(j,i)}$. First, we consider the case two index pairs are identical. We see from Eq. (19a) that there is no $\chi_{(i,j)}$ on the right side, so $\mathcal{W}_{(i,j),(i,j)}=0$. Next, we consider the case none of indices in one index pair is equal to any in the other, i.e., $i\neq p,q$ and $j\neq p,q$. It is obvious that no $\chi_{(p,q)}$ appears in the summations on the right side of Eq. (19a), which implies $\mathcal{W}_{(i,j),(p,q)}=0$. Similarly, we have $\mathcal{W}_{(p,q),(i,j)}=0$. Last, we consider the case in which one index in one index pair is equal to one index in another index pair but the remaining two indices from two index pair are not equal. Without loss of generality, we assume $i=p$ and $j\neq q$. From Eq. (19a), we have

$$\frac{\mathrm{d}\chi_{(i,j)}}{\mathrm{d}t} = \cdots - D_{jq}\chi_{(i,q)} - \cdots = \cdots - D_{jq}\chi_{(p,q)} - \cdots,$$

where we have intentionally isolated the relevant term from the second summation and the last equality is due to $i=p$. Similarly, from Eq. (19b), we have

$$\frac{\mathrm{d}\chi_{(p,q)}}{\mathrm{d}t} = \cdots - D_{qj}\chi_{(p,j)} - \cdots = \cdots - D_{qj}\chi_{(i,j)} - \cdots.$$

The above two equations imply that $\mathcal{W}_{(i,j),(p,q)} = -\mathcal{W}_{(p,q),(i,j)}$. Similar arguments apply to other cases. This completes the proof. □

3.2. Error analysis

In this section, we will consider the convergence of the solution obtained by the DyBO formulation (15) to the original SPDE (1). Theorem 3.2 gives the error analysis of the DyBO formulation.

Theorem 3.2 (*The consistency between the DyBO formulation and the original SPDE*). *The stochastic solution of system (15) satisfies the following modified SPDE*

$$\frac{\partial \tilde{u}}{\partial t} = \mathcal{L}\tilde{u} + e_m, \tag{20}$$

where e_m is the error due to the m-term truncation and

$$e_m = -\Pi_{\mathbf{Y}}(\Pi_{\mathbf{U}}(\tilde{\mathcal{L}}\tilde{u})). \tag{21}$$

Proof. We show consistency by computing directly from Eqs. (15b) and (15c)

$$\mathbf{U}\frac{\mathrm{d}\mathbf{Y}^T}{\mathrm{d}t} = \tilde{\mathcal{L}}\tilde{u} + \mathbf{U}\mathbf{D}^T\mathbf{Y}^T - (\tilde{\mathcal{L}}\tilde{u} - \mathbf{U}\boldsymbol{\Lambda}_{\mathbf{U}}^{-1}\left\langle \mathbf{U}^T, \tilde{\mathcal{L}}\tilde{u}\right\rangle) - \mathbf{U}\boldsymbol{\Lambda}_{\mathbf{U}}^{-1}\left\langle \mathbf{U}^T, \mathbb{E}\left[\tilde{\mathcal{L}}\tilde{u}\mathbf{Y}\right]\right\rangle\mathbf{Y}^T,$$
$$\frac{\partial \mathbf{U}}{\partial t}\mathbf{Y}^T = \mathbf{U}\mathbf{C}\mathbf{Y}^T + \mathbf{Y}\mathbb{E}\left[\tilde{\mathcal{L}}\tilde{u}\mathbf{Y}^T\right] - \mathbf{Y}\left\langle \mathbb{E}\left[\tilde{\mathcal{L}}\tilde{u}\mathbf{Y}^T\right], \mathbf{U}\right\rangle\boldsymbol{\Lambda}_{\mathbf{U}}^{-1}\mathbf{U}^T.$$

Combining the above two, we have

$$\mathbf{U}\frac{\mathrm{d}\mathbf{Y}^T}{\mathrm{d}t} + \frac{\partial \mathbf{U}}{\partial t}\mathbf{Y}^T = \tilde{\mathcal{L}}\tilde{u} + e_m,$$

where

$$\begin{aligned} e_m &= -(\tilde{\mathcal{L}}\tilde{u} - \mathbf{U}\boldsymbol{\Lambda}_{\mathbf{U}}^{-1}\left\langle \mathbf{U}^T, \tilde{\mathcal{L}}\tilde{u}\right\rangle) + \mathbf{U}(\mathbf{D}^T + \mathbf{C})\mathbf{Y}^T - U\boldsymbol{\Lambda}_{\mathbf{U}}^{-1}\left\langle \mathbf{U}^T, \mathbb{E}\left[\tilde{\mathcal{L}}\tilde{u}\mathbf{Y}\right]\right\rangle\mathbf{Y}^T \\ &= -(\tilde{\mathcal{L}}\tilde{u} - \mathbf{U}\boldsymbol{\Lambda}_{\mathbf{U}}^{-1}\left\langle \mathbf{U}^T, \tilde{\mathcal{L}}\tilde{u}\right\rangle) + \mathbb{E}\left[(\tilde{\mathcal{L}}\tilde{u} - \mathbf{U}\boldsymbol{\Lambda}_{\mathbf{U}}^{-1}\left\langle \mathbf{U}^T, \tilde{\mathcal{L}}\tilde{u}\right\rangle)\mathbf{Y}\right]\mathbf{Y}^T, \end{aligned}$$

where Eq. (13c) has been used in deriving the first equality. By noticing $\tilde{\mathcal{L}}\tilde{u} = \mathcal{L}\tilde{u} - \mathbb{E}[\mathcal{L}\tilde{u}]$, we prove Eq. (20). □

Remark 3.2. According to Theorem 3.1, the bi-orthogonality of **U** and **Y** are preserved for all time. Because both Hilbert space $\mathbb{L}^2(\mathcal{D})$ and $\mathbb{L}^2(\Omega)$ are separable, the spatial basis **U** and the stochastic basis **Y** become a complete basis for $\mathbb{L}^2(\mathcal{D})$ and $\mathbb{L}^2(\Omega)$ as $m \to +\infty$, respectively, which implies $\lim_{m\to+\infty} e_m = 0$.

Next we consider a special case where the differential operator $\mathcal{L}$ is deterministic and linear, such as $\mathcal{L}v = c(x)\frac{\partial v}{\partial x}$, or $\mathcal{L}v = -\frac{\partial}{\partial x_i}(a_{ij}(x)\frac{\partial v}{\partial x_j})$, where $c(x)$ and $(a_{ij}(x))$ are deterministic functions. Only initial conditions are assumed to be random, i.e., the randomness propagates into the system only through initial conditions.

Corollary 3.3. *Let the differential operator $\mathcal{L}$ be deterministic and linear. The residual in Eq. (20) is zero for all time, i.e.,*

$$e_m(t) \equiv 0, \quad t > 0.$$

Proof. This can be seen by directly computing the truncation error e_m. First we substitute $\tilde{\mathcal{L}}\tilde{u} = \mathcal{L}\tilde{u} - \mathbb{E}[\mathcal{L}\tilde{u}]$ into Eq. (21),

$$e_m = -\Pi_{\mathbf{Y}}(\mathcal{L}\tilde{u} - \mathbb{E}[\mathcal{L}\tilde{u}] - \mathbf{U}\boldsymbol{\Lambda}_{\mathbf{U}}^{-1}\left\langle \mathbf{U}^T, \mathcal{L}\tilde{u} - \mathbb{E}[\mathcal{L}\tilde{u}]\right\rangle).$$

Since the differential operator $\mathcal{L}$ is deterministic and linear, we have $\mathcal{L}\tilde{u} = \mathcal{L}\bar{u} + \mathcal{L}\mathbf{U}\mathbf{Y}^T$, where $\mathcal{L}\mathbf{U} = (\mathcal{L}u_1, \mathcal{L}u_2, \cdots, \mathcal{L}u_m)$. This gives

$$\begin{aligned} e_m &= -\Pi_{\mathbf{Y}}(\mathcal{L}\bar{u} + \mathcal{L}\mathbf{U}\mathbf{Y}^T - \mathbb{E}\left[\mathcal{L}\bar{u} + \mathcal{L}\mathbf{U}\mathbf{Y}^T\right] - \mathbf{U}\boldsymbol{\Lambda}_{\mathbf{U}}^{-1}\left\langle \mathbf{U}^T, \mathcal{L}\tilde{u} - \mathbb{E}[\mathcal{L}\tilde{u}]\right\rangle) = -\Pi_{\mathbf{Y}}(\mathcal{L}\mathbf{U}\mathbf{Y}^T - \mathbf{U}\boldsymbol{\Lambda}_{\mathbf{U}}^{-1}\left\langle \mathbf{U}^T, \mathcal{L}\mathbf{U}\right\rangle\mathbf{Y}^T) \\ &= -\Pi_{\mathbf{Y}}(\mathbf{Y}(\mathcal{L}\mathbf{U}^T - \left\langle \mathcal{L}\mathbf{U}^T, \mathbf{U}\right\rangle\boldsymbol{\Lambda}_{\mathbf{U}}^{-1}\mathbf{U}^T)) = 0. \end{aligned}$$

The last line is due to the orthogonal complementary project. □

The above corollary implies that DyBO is exact if the randomness can be expressed in a finite-term KL expansion. The next corollary concerns a slightly different case where the differential operator $\mathcal{L}$ is affine in the sense that $\mathcal{L}u = \mathcal{L}\mathring{u} + f(x,t,\omega)$ and the differential operator $\mathcal{L}^\circ$ is linear and deterministic. The stochastic force $f(\cdot,t,\cdot) \in \mathbb{L}^2(\mathcal{D}\times\Omega)$ for all t.

Corollary 3.4. *If the differential operator $\mathcal{L}$ is affine, i.e., $\mathcal{L}u = \mathcal{L}\mathring{u} + f(x,t,\omega)$, and f is a second-order stochastic process at each fixed time t, the residual in Eq. (21) is given below*

$$e_m = -\Pi_{\mathbf{Y}}\Pi_{\mathbf{U}}(f).$$

Proof. Again by directly computing, we have by the linearity of the differential operator $\mathcal{L}^\circ$

$$\mathcal{L}\tilde{u} = \mathcal{L}\mathring{\tilde{u}} + \mathcal{L}\mathring{\mathbf{U}}\mathbf{Y}^T + f.$$

Simple calculation shows that

$$\tilde{\mathcal{L}}\tilde{u} = \mathcal{L}\tilde{u} - \mathbb{E}[\mathcal{L}\tilde{u}] = \mathcal{L}\mathring{\mathbf{U}}\mathbf{Y}^T + f - \mathbb{E}[f].$$

Substituting into Eq. (21), we complete the proof. □

Remark 3.5. For this special case, Corollary 3.4 implies that numerical solutions are accurate as long as the spatial basis **U** and the stochastic basis **Y** provide good approximations to the external forcing term f, which is not surprising at all.

4. Numerical implementation

4.1. Representation of stochastic basis Y

The DyBO formulation (15) is a combination of deterministic PDEs (15a) and (15b) and SODEs (15c). For the deterministic PDEs in the DyBO formulation, we can apply suitable spatial discretization schemes and numerical integrators to solve them numerically. One of the conceptual difficulties, from the viewpoint of the classical numerical PDEs, involves representations of random variables or functions defined on abstract probability space Ω. Essentially, there are three ways to represent numerically stochastic basis $\mathbf{Y}(\omega,t)$: ensemble representations in sampling methods, such as Monte carlo method, sparse grid based stochastic collocation method [1,8] and spectral representations, such as the generalized Polynomial Chaos method [53,54,50,27,33] or Wavelet based Chaos method [35].

4.1.1. Ensemble representation (DyBO-MC)

In the MC method framework, the stochastic basis $\mathbf{Y}(\omega,t)$ are represented by an ensemble of realizations, i.e.,

$$\mathbf{Y}(\omega,t) \approx \{\mathbf{Y}(\omega_1,t), \mathbf{Y}(\omega_2,t), \mathbf{Y}(\omega_3,t), \cdots, \mathbf{Y}(\omega_{N_r},t)\},$$

where N_r is the total number of realizations. Then the expectations in the DyBO formulation (15) can be replaced by ensemble averages, i.e.,

$$\frac{\partial \bar{u}}{\partial t}(x,t) = \frac{1}{N_r}\sum_{i=1}^{N_r}\mathcal{L}\tilde{u}(x,t,\omega_i), \tag{22a}$$

$$\frac{\partial \mathbf{U}}{\partial t}(x,t) = -\mathbf{U}(x,t)\mathbf{D}(t)^T + \frac{1}{N_r}\sum_{i=1}^{N_r}\tilde{\mathcal{L}}\tilde{u}(x,t,\omega_i)\mathbf{Y}(\omega_i,t), \tag{22b}$$

$$\frac{\mathrm{d}\mathbf{Y}}{\mathrm{d}t}(\omega_i,t) = -\mathbf{Y}(\omega_i,t)\mathbf{C}(t)^T + \left\langle \tilde{\mathcal{L}}\tilde{u}(x,t,\omega_i), \mathbf{U}(x,t)\right\rangle \mathbf{\Lambda}_{\mathbf{U}}(t)^{-1}, \tag{22c}$$

where $\mathbf{C}(t)$ and $\mathbf{D}(t)$ can be solved from (14) with

$$G_*(\bar{u},\mathbf{U},\mathbf{Y}) = \mathbf{\Lambda}_{\mathbf{U}}^{-1}\left\langle \mathbf{U}^T, \frac{1}{N_r}\sum_{i=1}^{N_r}\tilde{\mathcal{L}}\tilde{u}(x,t,\omega_i)\mathbf{Y}(\omega_i,t)\right\rangle \tag{23}$$

and

$$\tilde{\mathcal{L}}\tilde{u}(x,t,\omega_i) = \mathcal{L}\tilde{u}(x,t,\omega_i) - \frac{1}{N_r}\sum_{i=1}^{N_r}\mathcal{L}\tilde{u}(x,t,\omega_i). \tag{24}$$

The above system is the MC version of DyBO method and we denote it as DyBO-MC. Close examinations reveal that Eq. (22a) for expectation and Eq. (22b) for spatial basis are only solved once for all the realizations at each time iteration while Eq. (22c) for the stochastic basis is decoupled from realization to realization and can be solved simultaneously across all realizations. In this sense, we see that DyBO-MC is *semi-sampling* and it preserves some desirable features of MC method, for example, the convergence rate does not depend on stochastic dimensionality and the solution process of $Y(\omega_i,t)$'s are decoupled. Clearly, not only the number of realizations, but also how these realizations $\{\omega_i\}_{i=1}^{N_r}$ are chosen in Ω affects the numerical accuracy and the efficiency. Quasi Monte Carlo method [42,40], variance reduction and other techniques may be combined into DyBO-MC to further improve its efficiency and accuracy. However, the disadvantage of MC method is its slow convergence. Developing effective sampling version of DyBO method such as the multi-level Monte Carlo method [24] is currently under investigation.

4.1.2. Spectral representation (DyBO-gPC)

In many physical and engineering problems, randomness generally comes from various independent sources, so randomness in SPDE (1) is often given in terms of independent random variables $\xi_i(\omega)$. Throughout this paper, we assume only a finite number of independent random variables are involved, i.e., $\boldsymbol{\xi}(\omega) = (\xi_1(\omega), \xi_2(\omega), \cdots, \xi_r(\omega))$, where r is the number of such random variables. Without loss of generality, we can further assume they all have identical distribution $\rho(\cdot)$. Thus, the solution of SPDE (1) is a functional of these random variables, i.e., $u(x,t,\omega) = u(x,t,\boldsymbol{\xi}(\omega))$. When SPDE is driven by some known stochastic process, such as Brownian Motion B_t, by Cameron-Martin theorem [9], the stochastic solution can be approximated by a functional of identical independent standard Gaussian variables, i.e., $u(x,t,\omega) \approx u(x,t,\boldsymbol{\xi}(\omega))$ with ξ_i being a standard normal random variable.

In this paper, we only consider the case where randomness is given in terms of independent standard Gaussian random variables, i.e., $\xi_i \sim \mathcal{N}(0,1)$ and $\mathbf{H}$ are a set of tensor products of Hermite polynomials. In this case, the method described above is also known as the Wiener-Chaos Expansion [51,9,12,13,27]. When the distribution of ξ_i is not Gaussian, the discussions remain almost identical and the major difference is the set of orthogonal polynomials.

We denote by $\{\mathrm{H}_i(\xi)\}_{i=1}^{\infty}$ the one-dimensional polynomials orthogonal to each other with respect to the common distribution $\rho(z)$, i.e.,

$$\int_{-\infty}^{\infty}\mathrm{H}_i(\xi)\mathrm{H}_j(\xi)\rho(\xi)d\xi = \delta_{ij}.$$

For some common distributions, such as Gaussian or uniform distribution, such polynomial sets are well-known and well-studied, many of which fall in the Ashley scheme, see [53]. For general distributions, such polynomial sets can be obtained by numerical methods, see [50]. Furthermore, by a tensor product representation, we can use the one-dimensional polynomial $\mathrm{H}_i(\xi)$ to construct a complete orthonormal basis $\mathbf{H}_{\boldsymbol{\alpha}}(\boldsymbol{\xi})$'s of $\mathbb{L}^2(\Omega)$ as follows

$$\mathbf{H}_{\boldsymbol{\alpha}}(\boldsymbol{\xi}) = \prod_{i=1}^{r}\mathrm{H}_{\alpha_i}(\xi_i), \quad \boldsymbol{\alpha} \in \mathfrak{J}_r^{\infty},$$

where $\boldsymbol{\alpha}$ is a multi-index, i.e., a row vector of non-negative integers,

$$\boldsymbol{\alpha} = (\alpha_1, \alpha_2, \cdots, \alpha_r) \quad \alpha_i \in \mathbb{N}, \quad \alpha_i \geqslant 0,\ i = 1,2,\cdots,r$$

and $\mathfrak{J}_r^{\infty}$ is a multi-index set of countable cardinality,

$$\mathfrak{J}_r^\infty = \{\boldsymbol{\alpha} = (\alpha_1, \alpha_2, \cdots, \alpha_r) \,|\, \alpha_i \geqslant 0, \alpha_i \in \mathbb{N}\} \setminus \{0\}.$$

We have intentionally removed the zero multi-index corresponding to $\mathbf{H}_0(\xi) = 1$ since it is associated with the mean of the stochastic solution and it is better to deal with it separately according to our experience. When no ambiguity arises, we simply write the multi-index set $\mathfrak{J}_r^\infty$ as $\mathfrak{J}^\infty$. Clearly, the cardinality of $\mathfrak{J}_r^\infty$ is infinite. For the purpose of numerical computations, we prefer a polynomial set of finite size. There are many choices of truncations, such as the set of polynomials whose total orders are at most p, i.e.,

$$\mathfrak{J}_r^p = \left\{ \boldsymbol{\alpha} \,|\, \boldsymbol{\alpha} = (\alpha_1, \alpha_2, \cdots, \alpha_r), \alpha_i \geqslant 0, \alpha_i \in \mathbb{N}, |\alpha| = \sum_{i=1}^{r} \alpha_i \leqslant p \right\} \setminus \{0\}$$

and sparse truncations proposed in [27], see also Luo's thesis [32]. Again, we may simply write such a truncated set as $\mathfrak{J}$ when no ambiguity arises. The cardinality of $\mathfrak{J}$, or the total number of polynomial basis functions, denoted by $N_p = |\mathfrak{J}|$, is equal to $\frac{(p+r)!}{p!r!}$. As we can see, N_p grows exponentially fast as p and r increase. This is also known as the curse of dimensionality.

By the Cameron–Martin theorem [9], we know that the solution of SPDE (1) admits a generalized Polynomial Chaos expansion (gPCE)

$$u(x,t,\omega) = \bar{v}(x,t) + \sum_{\boldsymbol{\alpha}\in\mathfrak{J}^\infty} v_{\boldsymbol{\alpha}}(x,t)\mathbf{H}_{\boldsymbol{\alpha}}(\xi(\omega)) \approx \bar{v}(x,t) + \sum_{\boldsymbol{\alpha}\in\mathfrak{J}} v_{\boldsymbol{\alpha}}(x,t)\mathbf{H}_{\boldsymbol{\alpha}}(\xi(\omega)). \tag{25}$$

If we write

$$\mathbf{H}_{\mathfrak{J}}(\xi) = (\mathbf{H}_{\boldsymbol{\alpha}_1}(\xi), \mathbf{H}_{\boldsymbol{\alpha}_2}(\xi), \cdots, \mathbf{H}_{\boldsymbol{\alpha}_{N_p}}(\xi))_{\boldsymbol{\alpha}_i\in\mathfrak{J}},$$
$$\mathbf{V}(x,t) = (v_{\boldsymbol{\alpha}_1}(x,t), v_{\boldsymbol{\alpha}_2}(x,t), \cdots, v_{\boldsymbol{\alpha}_{N_p}}(x,t))_{\boldsymbol{\alpha}_i\in\mathfrak{J}},$$

both of which are row vectors, the above gPCE can be compactly written in a vector form

$$u^{\mathrm{gPC}}(x,t,\omega) = v(x,t,\omega) = \bar{v}(x,t) + \mathbf{V}(x,t)\mathbf{H}(\xi)^T. \tag{26}$$

By substituting the above gPCE into Eq. (1a), it is easy to derive the gPC formulation for SPDE (1),

$$\frac{\partial \bar{v}}{\partial t} = \mathbb{E}[\mathcal{L}v], \tag{27a}$$
$$\frac{\partial \mathbf{V}}{\partial t} = \mathbb{E}\big[\tilde{\mathcal{L}}v\mathbf{H}\big]. \tag{27b}$$

Now, we turn our attention to the gPC version of DyBO formulation (DyBO-gPC). The Cameron–Martin theorem also implies the stochastic basis $Y_i(\omega,t)$'s in the KL expansion (7) can be approximated by the linear combination of polynomials chaos, i.e.,

$$Y_i(\omega,t) = \sum_{\boldsymbol{\alpha}\in\mathfrak{J}} \mathbf{H}_{\boldsymbol{\alpha}}(\xi(\omega))A_{\boldsymbol{\alpha}i}(t), \quad i = 1,2,\cdots,m, \tag{28}$$

or in a matrix form,

$$\mathbf{Y}(\omega,t) = \mathbf{H}(\xi(\omega))\mathbf{A}, \tag{29}$$

where $\mathbf{A} \in \mathbb{R}^{N_p\times m}$. The expansion (7) now reads

$$\tilde{u} = \bar{u} + \mathbf{U}\mathbf{A}^T\mathbf{H}^T.$$

We can derive equations for $\bar{u}, \mathbf{U}$ and $\mathbf{A}$, instead of $\bar{u}, \mathbf{U}$ and $\mathbf{Y}$. In other words, the stochastic basis $\mathbf{Y}$ are identified with a matrix $\mathbf{A} \in \mathbb{R}^{N_p\times m}$ in DyBO-gPC. Substituting Eq. (29) into Eq. (15c) and using the identity $\mathbb{E}\left[\mathbf{H}^T\mathbf{H}\right] = \mathbf{I}$, we get the DyBO-gPC formulation of SPDE (1),

$$\frac{\partial \bar{u}}{\partial t} = \mathbb{E}[\mathcal{L}\tilde{u}], \tag{30a}$$
$$\frac{\partial \mathbf{U}}{\partial t} = -\mathbf{U}\mathbf{D}^T + \mathbb{E}\big[\tilde{\mathcal{L}}\tilde{u}\mathbf{H}\big]\mathbf{A}, \tag{30b}$$
$$\frac{\mathrm{d}\mathbf{A}}{\mathrm{d}t} = -\mathbf{A}\mathbf{C}^T + \left\langle \mathbb{E}\left[\mathbf{H}^T\tilde{\mathcal{L}}\tilde{u}\right], \mathbf{U}\right\rangle \boldsymbol{\Lambda}_{\mathbf{U}}^{-1}, \tag{30c}$$

where $\mathbf{C}(t)$ and $\mathbf{D}(t)$ can be solved from (14) with

$$G_*(\bar{u},\mathbf{U},\mathbf{Y}) = \boldsymbol{\Lambda}_{\mathbf{U}}^{-1}\left\langle \mathbf{U}^T, \mathbb{E}\big[\tilde{\mathcal{L}}\tilde{u}\mathbf{Y}\big]\right\rangle = \boldsymbol{\Lambda}_{\mathbf{U}}^{-1}\left\langle \mathbf{U}^T, \mathbb{E}\big[\tilde{\mathcal{L}}\tilde{u}\mathbf{H}\big]\right\rangle \mathbf{A}. \tag{31}$$

By solving the system (30), we have an approximate solution to SPDE (1)

$$u^{\text{DyBO-gPC}} = \bar{u} + \mathbf{U}\mathbf{A}^T\mathbf{H}^T,$$

or simply u^{DyBO} when no ambiguity arises.

4.1.3. gSC representation (DyBO-gSC)

In our DyBO-gPC method, the stochastic process $Y_i(\xi(\omega),t)$ is projected onto the gPC basis $\mathbf{H}$ and replaced by gPC coefficients, i.e., $A_{\alpha i}$, which can be computed by

$$A_{\alpha i} = \mathbb{E}[Y_i(\omega)\mathbf{H}_\alpha(\xi(\omega))].$$

Numerically, the above integral can be evaluated with high accuracy on some sparse grid. In other words, the stochastic basis $\mathbf{Y}$ can also be represented as an ensemble of realizations $\mathbf{Y}(\omega_i)$ where $\xi(\omega_i)$'s are nodes from some sparse grid and associated with certain weight w_i. The gSC version of DyBO formulation, which we denote as DyBO-gSC, is

$$\frac{\partial \bar{u}}{\partial t}(x,t) = \sum_{i=1}^{N_s} w_i \mathcal{L}\tilde{u}(x,t,\omega_i), \tag{32a}$$

$$\frac{\partial \mathbf{U}}{\partial t}(x,t) = -\mathbf{U}(x,t)\mathbf{D}(t)^T + \sum_{i=1}^{N_s} w_i \tilde{\mathcal{L}}\tilde{u}(x,t,\omega_i)\mathbf{Y}(\omega_i,t), \tag{32b}$$

$$\frac{\mathrm{d}\mathbf{Y}}{\mathrm{d}t}(\omega_i,t) = -\mathbf{Y}(\omega_i,t)\mathbf{C}(t)^T + \langle \tilde{\mathcal{L}}\tilde{u}(x,t,\omega_i), \mathbf{U}(x,t)\rangle \mathbf{\Lambda}_{\mathbf{U}}(t)^{-1}, \quad i = 1,2,\ldots,N_s, \tag{32c}$$

where $\{\omega_i\}_{i=1}^{N_s}$ are the sparse grid points, $\{w_i\}_{i=1}^{N_s}$ are the weight, N_s is the number of sparse grid points and $\mathbf{C}(t), \mathbf{D}(t)$ can be solved from (14) with

$$G_*(\bar{u},\mathbf{U},\mathbf{Y}) = \mathbf{\Lambda}_{\mathbf{U}}^{-1}\left\langle \mathbf{U}^T, \sum_{i=1}^{N_s} w_i \tilde{\mathcal{L}}\tilde{u}(x,t,\omega_i)\mathbf{Y}(\omega_i,t)\right\rangle. \tag{33}$$

The primary focus of this paper is on DyBO-gPC methods. We will provide details and numerical examples of DyBO-gSC methods in our future work.

4.2. Eigenvalue crossings

As the system evolves, eigenvalues of different basis in the KL expansion of the SPDE solution may increase or decrease. Some of them may approach each other at some time, cross and then separate as illustrated in Fig. 2. In the figure, λ_1 and λ_2 cross each other at t_1^* and λ_1 and λ_3 cross each other at t_2^*. In this case, if $\mathbf{C}$ and $\mathbf{D}$ continue to be solved from the linear system (13) via (14), numerical errors will pollute the results. Here, we propose to freeze $\mathbf{U}$ or $\mathbf{Y}$ temporarily for a short time and continue to evolve the system using different equations as derived below. At the end of this short duration, the solution is recast into the bi-orthogonal form via the KL expansion, which can be achieved efficiently since $\mathbf{U}$ or $\mathbf{Y}$ is still kept orthogonal in this short duration. We are also currently exploring alternative approach to overcome the eigenvalue crossing problem, and will report our result in a subsequent paper.

In order to apply the above strategy, we have to be able to detect that two eigenvalues may potentially cross each other in the near future. There are several ways to detect such crossing. Here we propose to monitor the following quantity

$$\tau = \min_{i\neq j} \frac{|\lambda_i - \lambda_j|}{\max(\lambda_i,\lambda_j)}. \tag{34}$$

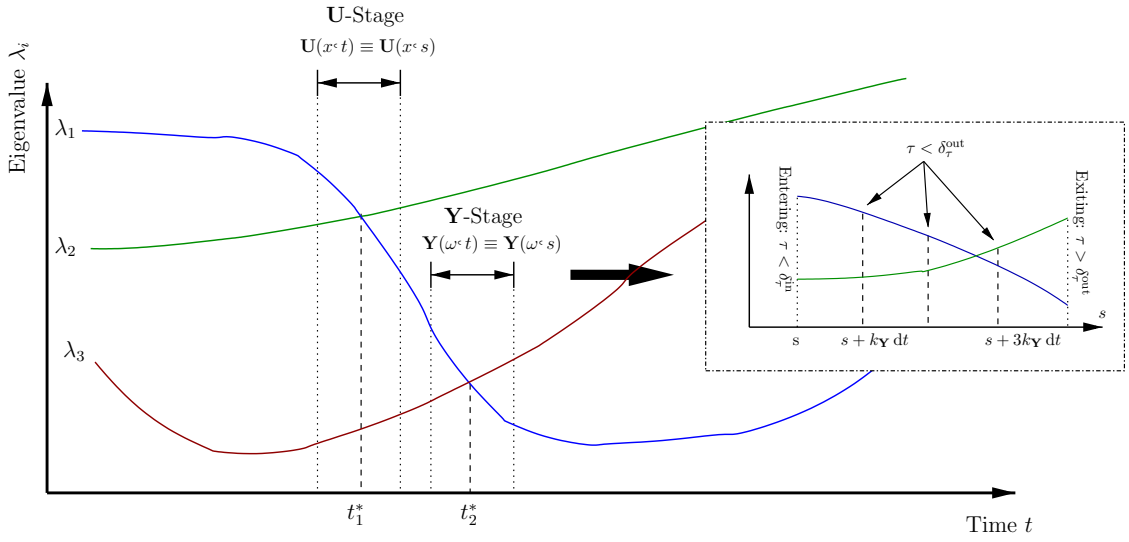

Fig. 2. Illustration of Eigenvalue Crossing.

Once this quantity drops below certain threshold $\delta_\tau^{\text{in}} \in (0,1)$, we adopt the algorithm of freezing $\mathbf{U}$ or $\mathbf{Y}$ to evolve the system and continue to monitor this quantity τ. When τ exceeds some pre-specified threshold $\delta_\tau^{\text{out}} \in (0,1)$, the algorithm recasts the solution in the bi-orthogonal form via an efficient algorithm detailed in the next two sub-sections and continues to evolve the DyBO system. Threshold δ_τ^{in} and δ_τ^{out} may be problem-dependent. In our numerical experiments, we found $\delta_\tau^{\text{in}} = 1\%$ and $\delta_\tau^{\text{out}} = 1\%$ gave accurate results.

Here we only describe the basic idea of freezing stochastic basis $\mathbf{Y}$ or $\mathbf{Y}$-Stage algorithm. The method of freezing the spatial basis $\mathbf{U}$ or U-Stage algorithm can be obtained analogously, see [10] for more details. Suppose at some time $t = s$, potential eigenvalue crossing is detected and the stochastic basis $\mathbf{Y}$ are frozen for a short duration Δs, i.e., $\mathbf{Y}(\omega,t) \equiv \mathbf{Y}(\omega,s)$ for $t \in [s, s+\Delta s]$, which we call $\mathbf{Y}$-stage. Because $\mathbf{Y}$ are orthonormal, the solution of SPDE (1) admits the following approximation of a truncated expansion.

$$\tilde{u}(x,t,\omega) = \bar{u}(x,t) + \sum_{i=1}^{m} u_i(x,t) Y_i(\omega,s) = \bar{u}(x,t) + \mathbf{U}(x,t)\mathbf{Y}(\omega,s)^T. \tag{35}$$

It is easy to derive a new evolution system for this stage,

$$\frac{\partial \bar{u}}{\partial t} = \mathbb{E}[\mathcal{L}\tilde{u}], \tag{36a}$$

$$\frac{\partial \mathbf{U}}{\partial t} = \mathbb{E}\left[\tilde{\mathcal{L}}\tilde{u}\mathbf{Y}\right]. \tag{36b}$$

During this stage, $\mathbf{Y}$ is unchanged and orthogonal, but $\mathbf{U}$ changes in time and would not maintain its orthogonality. The solution is no longer bi-orthogonal, so eigenvalues cannot be computed via $\lambda_i = \|u_i\|^2_{\mathbb{L}^2(\mathcal{D})}$ any more. Next, we derive formula for eigenvalues in this stage and then show how the solutions are recast into the bi-orthogonal form at the end of the stage, i.e., $t = s + \Delta s$.

The covariance function can be computed as

$$\text{Cov}_{\tilde{u}}(x,y) = \mathbb{E}[(\tilde{u}(x) - \bar{u}(x))(\tilde{u}(y) - \bar{u}(y))] = \mathbb{E}\left[\mathbf{U}(x)\mathbf{Y}^T\mathbf{Y}\mathbf{U}^T(y)\right] = \mathbf{U}(x)\mathbf{U}^T(y),$$

where t is omitted for simplicity and $\mathbb{E}\left[\mathbf{Y}^T\mathbf{Y}\right] = \mathbf{I}$ is used. By some stable orthogonalization procedures, such as the modified Gram-Schmidt algorithm, $\mathbf{U}(x)$ can be written as

$$\mathbf{U}(x) = \mathbf{Q}(x)\mathbf{R}, \tag{37}$$

where $\mathbf{Q}(x) = (q_1(x), q_2(x), \cdots, q_m(x)), q_i(x) \in \mathbb{L}^2(\mathcal{D})$ for $i = 1,2,\cdots,m$, $\left\langle \mathbf{Q}^T(x), \mathbf{Q}(x) \right\rangle = \mathbf{I}$ and $\mathbf{R} \in \mathbb{R}^{m\times m}$. Here $\mathbf{R}\mathbf{R}^T \in \mathbb{R}^{m\times m}$ is a positive definite symmetric matrix and its SVD decomposition reads

$$\mathbf{R}\mathbf{R}^T = \mathbf{W}\mathbf{\Lambda}_\mathbf{R}\mathbf{W}^T, \tag{38}$$

where $\mathbf{W} \in \mathbb{R}^{m\times m}$ is an orthonormal matrix, i.e., $\mathbf{W}\mathbf{W}^T = \mathbf{W}^T\mathbf{W} = \mathbf{I}$, and $\mathbf{\Lambda}_\mathbf{R}$ is a diagonal matrix with positive diagonal entries. The computational cost of $\mathbf{W}$ and $\mathbf{\Lambda}_\mathbf{R}$ is negligible compared to other parts of the algorithm. The covariance function can be rewritten as

$$\text{Cov}_{\tilde{u}}(x,y) = \mathbf{Q}(x)\mathbf{R}\mathbf{R}^T\mathbf{Q}^T(y) = \mathbf{Q}(x)\mathbf{W}\mathbf{\Lambda}_\mathbf{R}\mathbf{W}^T\mathbf{Q}^T(y).$$

Now, it is easy to see that the eigenfunctions of covariance function $\text{Cov}_{\tilde{u}}(x,y)$ are

$$\tilde{\mathbf{U}}(x) = \mathbf{Q}(x)\mathbf{W}\mathbf{\Lambda}_\mathbf{R}^{\frac{1}{2}}, \tag{39}$$

and eigenvalues are $\text{diag}(\mathbf{\Lambda}_\mathbf{R})$ because

$$\left\langle \tilde{\mathbf{U}}^T, \tilde{\mathbf{U}} \right\rangle = \left\langle \mathbf{\Lambda}_\mathbf{R}^{\frac{1}{2}}\mathbf{W}^T\mathbf{Q}^T, \mathbf{Q}\mathbf{W}\mathbf{\Lambda}_\mathbf{R}^{\frac{1}{2}} \right\rangle = \mathbf{\Lambda}_\mathbf{R},$$

where we have used the orthogonality of $\mathbf{Q}$ and $\mathbf{W}$. To compute $\tilde{\mathbf{Y}}$, we start with the identity

$$\tilde{\mathbf{Y}}\tilde{\mathbf{U}}^T = \mathbf{Y}\mathbf{U}^T,$$

and multiply row vector $\tilde{\mathbf{U}}$ on both sides from the right and take inner product $\langle\cdot,\cdot\rangle$,

$$\tilde{\mathbf{Y}}\left\langle \tilde{\mathbf{U}}^T, \tilde{\mathbf{U}} \right\rangle = \mathbf{Y}\left\langle \mathbf{U}^T, \tilde{\mathbf{U}} \right\rangle,$$

where

$$\left\langle \tilde{\mathbf{U}}^T, \tilde{\mathbf{U}} \right\rangle = \mathbf{\Lambda}_\mathbf{R},$$

$$\left\langle \mathbf{U}^T, \tilde{\mathbf{U}} \right\rangle = \left\langle \mathbf{R}^T\mathbf{Q}^T(x), \mathbf{Q}(x)\mathbf{W}\mathbf{\Lambda}_\mathbf{R}^{\frac{1}{2}} \right\rangle = \mathbf{R}^T\mathbf{W}\mathbf{\Lambda}_\mathbf{R}^{\frac{1}{2}}.$$

So we obtain the stochastic basis $\tilde{\mathbf{Y}}$, which is given by

$$\tilde{\mathbf{Y}} = \mathbf{Y}\mathbf{R}^T\mathbf{W}\boldsymbol{\Lambda}_{\mathbf{R}}^{-\frac{1}{2}}. \tag{40}$$

If a generalized polynomial basis $\mathbf{H}$ is adopted to represent $\mathbf{Y}$, we freeze $\mathbf{A}$ instead, i.e., $\mathbf{A}(t) \equiv \mathbf{A}(s)$ and the system (36) is replaced by

$$\frac{\partial \bar{u}}{\partial t} = \mathbb{E}[\mathcal{L}\tilde{u}], \tag{41a}$$

$$\frac{\partial \mathbf{U}}{\partial t} = \mathbb{E}\left[\tilde{\mathcal{L}}\tilde{u}\mathbf{H}\right]\mathbf{A}, \tag{41b}$$

where $\mathbf{A}(t) \equiv \mathbf{A}(s)$. At the exiting point, Eq. (40) is replaced by

$$\tilde{\mathbf{A}} = \mathbf{A}\mathbf{R}^T\mathbf{W}\boldsymbol{\Lambda}_{\mathbf{R}}^{-\frac{1}{2}}. \tag{42}$$

As we can see, the computation of eigenvalues in this stage is not trivial, so we do not want to compute τ every time iteration. Instead, τ is only evaluated every $k_{\mathbf{Y}}$ time steps to achieve a balance between computational efficiency and accuracy. See the zoom-in figure in Fig. 2 for illustration.

5. Numerical examples

Previous sections highlight the analytical aspects of the DyBO formulation and its numerical algorithm. In this section, we demonstrate the effectiveness of this method by several numerical examples with increasing level of difficulties, each of which emphasizes and verifies some of analytical results in the previous sections. In the first example, we consider a SPDE which is driven purely by stochastic forces. The purpose of this example is to show that the DyBO formulation tracks the KL expansion. Corollary 3.3 regarding the error propagation of the DyBO method is numerically verified in the second numerical example where a transport equation with a deterministic velocity and random initial conditions is considered. In the last example, we consider Burgers' equation driven by a stochastic force as an example of a nonlinear PDE driven by stochastic forces. We demonstrate the convergence of the DyBO method with respect to the number of basis pairs, m. In the second part of this paper [11], we will consider the more challenging Navier–Stokes equations and the Boussinesq approximation with random forcings. Some important numerical issues, such as adaptivity, parallelization and computational complexity, will be also studied in details.

5.1. SPDE purely driven by stochastic force

To study the convergence of our DyBO-gPC algorithms, it is desirable to construct a SPDE whose solution and KL expansion are known analytically. This would allow us to perform a thorough convergence study for our algorithm especially when we encounter eigenvalue crossings. In this example, we consider a SPDE which is purely driven by a stochastic force f, i.e., $\frac{\partial u}{\partial t} = \mathcal{L}u = f(x,t,\omega)$. The solution can be obtained by direct integration, i.e., $u(x,t,\omega) = u(x,0,\omega) + \int_0^t f(x,s,\omega)ds$. Specifically, in this section, we consider the SPDE

$$\frac{\partial u}{\partial t} = \mathcal{L}u = f(x,t,\boldsymbol{\xi}(\omega)), \quad x \in \mathcal{D} = [0,1], t \in [0,T], \tag{43}$$

where $\boldsymbol{\xi} = (\xi_1, \xi_2, \cdots, \xi_r)$ are independent standard Gaussian random variables, i.e., $\xi_i \sim \mathcal{N}(0,1), i = 1,2,\cdots,r$. The exact solution is constructed as follows

$$u(x,t,\boldsymbol{\xi}) = \bar{v}(x,t) + \mathbf{V}(x,t)\mathbf{Z}^T(\xi,t), \tag{44}$$

where $\mathbf{V}(x,t) = \mathbf{V}(\mathring{x})\mathbf{W}_{\mathbf{V}}(t)\boldsymbol{\Lambda}_{\mathbf{V}}^{\frac{1}{2}}(t), \mathbf{Z}(\xi,t) = \mathbf{Z}(\mathring{\xi})\mathbf{W}_{\mathbf{Z}}(t), \mathbf{V}(\mathring{x}) = (\mathring{v}_1(x), \cdots, \mathring{v}_m(x))$ with $\langle \mathring{v}_i(x), \mathring{v}_j(x)\rangle = \delta_{ij}$ and $\mathbf{Z}(\mathring{\xi}) = (Z_1(\xi), \cdots, Z_m(\xi))$ with $\mathbb{E}[Z_iZ_j] = \delta_{ij}$ for $i,j = 1,2,\cdots,m$. $\mathbf{W}_{\mathbf{V}}(t)$ and $\mathbf{W}_{\mathbf{Z}}(t)$ are m-by-m orthonormal matrices, and $\boldsymbol{\Lambda}_{\mathbf{V}}^{\frac{1}{2}}(t)$ is a diagonal matrix.

Clearly, the exact solution u is intentionally given in the form of its finite-term KL expansion and the diagonal entries of matrix $\boldsymbol{\Lambda}_{\mathbf{V}}(t)$ are its eigenvalues. By carefully choosing the eigenvalues, we can mimic various difficulties which may arise in more involved situations and devise corresponding strategies. The stochastic forcing term on the right hand side of Eq. (43) can be obtained by differentiating the exact solution, i.e.,

$$\mathcal{L}u = f = \frac{\partial \bar{v}}{\partial t} + \frac{\partial \mathbf{V}}{\partial t}\mathbf{Z}^T + \mathbf{V}\frac{\mathrm{d}\mathbf{Z}^T}{\mathrm{d}t}. \tag{45}$$

The initial condition of SPDE (40) can be obtained by simply setting $t = 0$ in Eq. (44). From the general DyBO-gPC formulation (15), simple calculations give the DyBO-gPC formulation for SPDE (43)

$$\frac{\partial \bar{u}}{\partial t} = \frac{\partial \bar{v}}{\partial t}, \tag{46a}$$

$$\frac{\partial \mathbf{U}}{\partial t} = -\mathbf{U}\mathbf{D}^T + (\frac{\partial \mathbf{V}}{\partial t}\mathbf{W}_\mathbf{Z}^T + \mathbf{V}\frac{\mathrm{d}\mathbf{W}_\mathbf{Z}^T}{\mathrm{d}t})\mathbb{E}\big[\mathbf{Z}^T\mathbf{H}\big]\mathbf{A}, \tag{46b}$$

$$\frac{\mathrm{d}\mathbf{A}}{\mathrm{d}t} = -\mathbf{A}\mathbf{C}^T + \mathbb{E}\Big[\mathbf{H}^T\mathbf{Z}\Big]\left\langle \mathbf{W}_\mathbf{Z}\frac{\partial \mathbf{V}^T}{\partial t} + \frac{\mathrm{d}\mathbf{W}_\mathbf{Z}}{\mathrm{d}t}\mathbf{V}^T, \mathbf{U}\right\rangle \mathbf{\Lambda}_\mathbf{U}^{-1}, \tag{46c}$$

and

$$G_*(u,\mathbf{U},\mathbf{A}) = \mathbf{\Lambda}_\mathbf{U}^{-1}\left\langle \mathbf{U}, \frac{\partial \mathbf{V}}{\partial t}\mathbf{W}_\mathbf{Z}^T + \mathbf{V}\frac{\mathrm{d}\mathbf{W}_\mathbf{Z}^T}{\mathrm{d}t}\right\rangle \mathbb{E}\big[\mathbf{Z}^T\mathbf{H}\big]\mathbf{A}.$$

The initial conditions are simply

$$\bar{u}(x,0) = \bar{v}(x,0), \quad \mathbf{U}(x,0) = \mathbf{V}(x,0), \quad \mathbf{A}(0) = \mathbb{E}\Big[\mathbf{H}^T\mathbf{Z}(\xi,0)\Big] = \mathbb{E}\Big[\mathbf{H}^T\mathbf{Z}\Big]\mathbf{W}_\mathbf{Z}(0).$$

In the event of eigenvalue crossings, we have the **Y**-stage system from (41),

$$\frac{\partial \bar{u}}{\partial t} = \frac{\partial \bar{v}}{\partial t}, \tag{47a}$$

$$\frac{\partial \mathbf{U}}{\partial t} = \left(\frac{\partial \mathbf{V}}{\partial t}\mathbf{W}_\mathbf{Z}^T + \mathbf{V}\frac{\mathrm{d}\mathbf{W}_\mathbf{Z}^T}{\mathrm{d}t}\right)\mathbb{E}\big[\mathbf{Z}^T\mathbf{H}\big]\mathbf{A}, \tag{47b}$$

or the **U**-stage system,

$$\frac{\partial \bar{u}}{\partial t} = \frac{\partial \bar{v}}{\partial t}, \tag{48a}$$

$$\frac{\mathrm{d}\mathbf{A}}{\mathrm{d}t} = \mathbb{E}\Big[\mathbf{H}^T\mathbf{Z}\Big]\left\langle \mathbf{W}_\mathbf{Z}\frac{\partial \mathbf{V}^T}{\partial t} + \frac{\mathrm{d}\mathbf{W}_\mathbf{Z}}{\mathrm{d}t}\mathbf{V}^T, \mathbf{U}\right\rangle \mathbf{\Lambda}_\mathbf{U}^{-1}. \tag{48b}$$

In the numerical examples presented in this section, we consider a small system $m = 3$ and use the following settings,

$$\mathbf{V}(\mathring{x}) = (\sqrt{2}\sin(\pi x), \sqrt{2}\sin(5\pi x), \sqrt{2}\sin(9\pi x)), \quad \mathbf{Z}(\mathring{x}) = (\mathrm{H}_1(\xi_1), \mathrm{H}_2(\xi_1), \mathrm{H}_3(\xi_1)),$$

$$\mathbf{W}_\mathbf{V}(t) = \mathrm{P}_\mathbf{V}\begin{pmatrix} \cos b_\mathbf{V} t & -\sin b_\mathbf{V} t & 0 \\ \sin b_\mathbf{V} t & \cos b_\mathbf{V} t & 0 \\ 0 & 0 & 1 \end{pmatrix}\mathrm{P}_\mathbf{V}^T, \quad \mathbf{W}_\mathbf{Z}(t) = \mathrm{P}_\mathbf{Z}\begin{pmatrix} \cos b_\mathbf{Z} t & -\sin b_\mathbf{Z} t & 0 \\ \sin b_\mathbf{Z} t & \cos b_\mathbf{Z} t & 0 \\ 0 & 0 & 1 \end{pmatrix}\mathrm{P}_\mathbf{Z}^T,$$

where $b_\mathbf{V} = 2.0, b_\mathbf{Z} = 2.0, \mathrm{P}_\mathbf{V}$ and $\mathrm{P}_\mathbf{Z}$ are two orthonormal matrices generated randomly, and $\mathbf{H}(\xi) = (\mathrm{H}_1(\xi_1), \mathrm{H}_2(\xi_1), \cdots, \mathrm{H}_5(\xi_1))$. Eigenvalues in the KL expansion of an SPDE solution may increase or decrease as time increases. Some of them may approach each other at some time, cross and then separate later. When two eigenvalues are close or equal to each other, numerical instability may arise in solving matrices **C** and **D** via (14). In Section 4.2, we have proposed a **U**-Stage by freezing the spatial basis **U** or a **Y**-Stage by freezing the stochastic basis **Y** temporarily to resolve this issue. Here, we demonstrate the success by incorporating such strategies into the DyBO algorithm. To this end, we choose $T = 1.2$ and eigenvalues

$$\mathbf{\Lambda}_\mathbf{V}^{\frac{1}{2}} = \mathrm{diag}(\sin 2\pi t + 2, \cos 2\pi t + 1.5, 1.8),$$

where eigenvalues cross each other at $t \approx 0.0675, 0.2015, 0.5320, 0.7985, 0.9650, 1.0675$, see Fig. 5.

In this numerical example, the time step $\Delta t = 1.0 \times 10^{-3}$ and $k_\mathbf{U} = 20$ in the **U**-stage, i.e., the exiting condition is checked every 20 time iterations when the system is in the **U**-stage. The mean $\mathbb{E}[u]$, the standard deviation (STD) $\sqrt{\mathrm{Var}(u)}$ and the three spatial basis in KLE at time $t = T$ are shown in Fig. 3 and Fig. 4, respectively. Clearly, the results given by DyBO almost perfectly match the exact ones with $\mathbb{L}^2$ relative errors of mean and STD below 10^{-10} since only the spatial and temporal discretizations contribute to the numerical errors in this example. In Fig. 5, eigenvalues are plotted as functions of time and zoom-in figures are given at $t = 0.0675$ and $t = 0.7985$ to show eigenvalue crossings and invoking of the **U**-stage algorithm.

We also check the deviation of the computed spatial and stochastic basis from the bi-orthogonality by monitoring $\frac{\langle u_i, u_j\rangle}{\|u_i\|_{\mathbb{L}^2(\mathcal{D})}\|u_j\|_{\mathbb{L}^2(\mathcal{D})}}$ for the spatial basis and $\mathbb{E}\big[Y_i Y_j\big]$ for the stochastic basis. The results are shown in Fig. 6. We observe that the deviation of the spatial basis from orthogonality is very small ($< 10^{-10}$) throughout the computation. Large deviations of the stochastic basis from the orthogonality only occur when eigenvalues cross each other since the DyBO algorithm is not designed to preserve the orthogonality of **Y** during the **U**-stage and orthogonality is only restored once the algorithm exits from the **U**-stage. We have also applied the **Y**-stage to overcome eigenvalue-crossing issues in this numerical examples and the results are very similar.

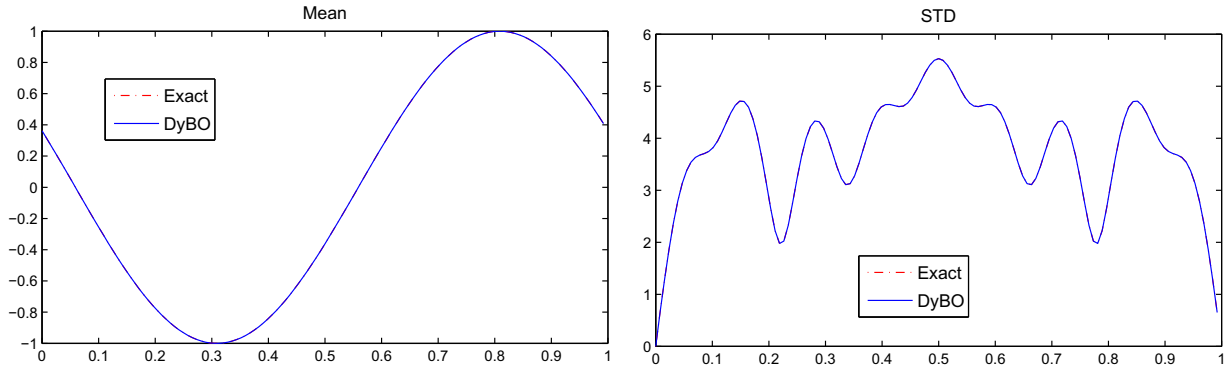

Fig. 3. Mean and STD computed by DyBO at time $t = 1.2$.

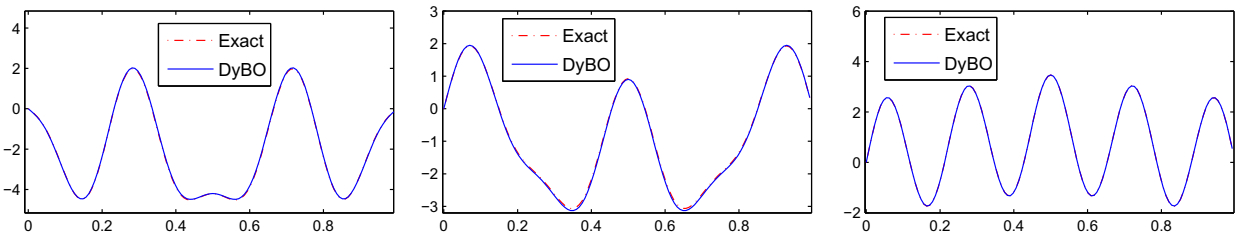

Fig. 4. The spatial basis $(u_1(x,t), u_2(x,t), u_3(x,t)$ from the left to the right) in KL expansion of SPDE solution computed by DyBO at time $t = 1.2$.

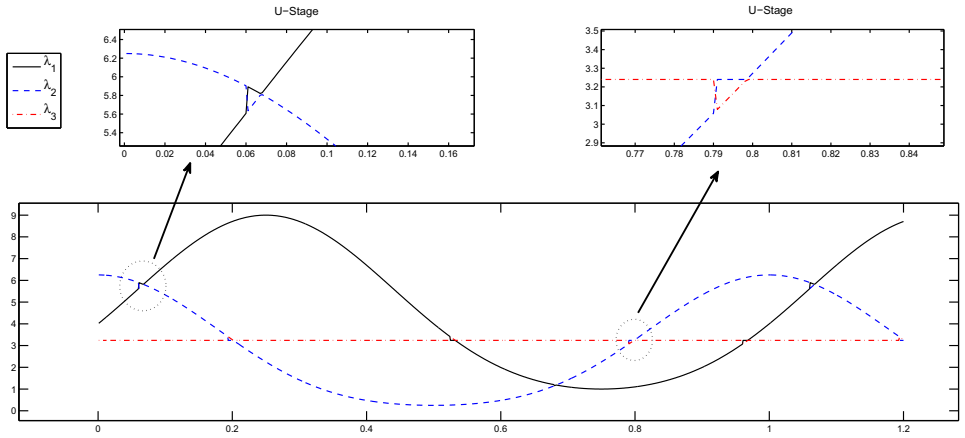

Fig. 5. Eigenvalues computed by DyBO. Two zoom-in figures are provided when eigenvalues cross.

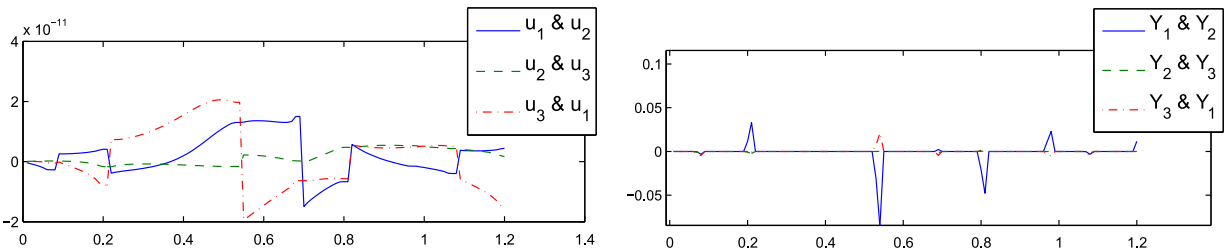

(a) Orthogonality of the spatial basis $\mathbf{U}(x^{\epsilon}t)$. (b) Orthogonality of the stochastic basis $\mathbf{Y}(\omega^{\epsilon}t)$.

Fig. 6. Bi-orthgonality of spatial and stochastic basis.

5.2. Linear deterministic differential operators with random initial conditions

In this section, we consider a linear PDE with random initial conditions, i.e., the differential operator $\mathcal{L}$ is deterministic and linear. For simplicity, we assume periodic boundary conditions.

$$\frac{\partial u}{\partial t} = \mathcal{L}u, \quad x \in [0,1],\ t \in [0,0.4], \tag{49a}$$

$$u(0,t,\boldsymbol{\xi}) = u(1,t,\boldsymbol{\xi}), \tag{49b}$$

$$u(x,0,\boldsymbol{\xi}) = u(\mathring{x},\boldsymbol{\xi}), \tag{49c}$$

where $\boldsymbol{\xi} = (\xi_1, \xi_2, \cdots, \xi_r)$ are independent standard Gaussian random variables.

Consider the gPC expansion of solution $u = \bar{v} + \mathbf{V}\mathbf{H}^T$. From Eq. (27), it is easy to obtain the gPC formulation of this SPDE,

$$\frac{\partial \bar{v}}{\partial t} = \mathcal{L}\bar{v}, \tag{50a}$$

$$\frac{\partial \mathbf{V}}{\partial t} = \mathcal{L}\mathbf{V}, \tag{50b}$$

where the initial conditions $\bar{v}(x,0) = \mathbb{E}[u]$ and $\mathbf{V}(x,0) = \mathbb{E}\left[u(\mathring{x})\mathbf{H}\right]$. Clearly, the gPC formulation (50) is linear and provides the exact solution to the original SPDE (49) if the finite-term gPC expansion of the initial condition is exact, i.e., $u \doteq \mathbb{E}[u] + \mathbb{E}\left[u\mathring{\mathbf{H}}\right]\mathbf{H}^T$.

Now consider the KL expansion of the solution, $u = \bar{u} + \mathbf{U}\mathbf{Y}^T = \bar{u} + \mathbf{U}\mathbf{A}^T\mathbf{H}^T$. From the general DyBO-gPC formulation (15), simple calculations give the DyBO-gPC formulation for the SPDE (49)

$$\frac{\partial \bar{u}}{\partial t} = \mathcal{L}\bar{u}, \tag{51a}$$

$$\frac{\partial \mathbf{U}}{\partial t} = -\mathbf{U}\mathbf{D}^T + \mathcal{L}\mathbf{U}, \tag{51b}$$

$$\frac{\mathrm{d}\mathbf{A}}{\mathrm{d}t} = -\mathbf{A}\mathbf{C}^T + \mathbf{A}\left\langle \mathcal{L}\mathbf{U}^T, \mathbf{U}\right\rangle \Lambda_{\mathbf{U}}^{-1}, \tag{51c}$$

where $\mathbf{C}$ and $\mathbf{D}$ can be computed via Eq. (14) from $G_* = \Lambda_{\mathbf{U}}^{-1}\left\langle \mathbf{U}^T, \mathcal{L}\mathbf{U}\right\rangle$.

If we compare the DyBO formulation (51) and the gPC formulation (51) for the linear SPDE (49), we observe the following interesting phenomenon. Although the original SPDE is linear and the gPC formulation remains linear, the DyBO formulation is clearly *not* linear. However, this is not surprising because KL expansion is not a linear procedure. On the other hand, the gPC expansion is indeed a linear procedure. As we argue in Section 3.2, our DyBO formulation essentially tracks the KL expansion of the exact solution. Therefore, the non-linearity of KLE must be naturally built into the DyBO formulation to enable such tracking.

Corollary 3.3 implies that the solution given by the DyBO formulation is exact if the initial condition u can be expressed exactly by a finite-term KL expansion. To verify this numerically, we consider a transport equation, i.e., $\mathcal{L} = -\sin(2\pi(x+2t))\frac{\partial}{\partial x}$ and the initial condition is a functional of three standard Gaussian random variables, i.e., $r = 3$,

$$u(\mathring{x},\boldsymbol{\xi}) = \cos(2\pi x) + (\sin(2\pi x), \frac{1}{2}\sin(4\pi x), \frac{1}{3}\sin(6\pi x))\mathbf{A}^T\mathbf{H}_{\mathfrak{J}}^T,$$

where $\mathfrak{J} = \{\boldsymbol{\alpha} \,|\, \boldsymbol{\alpha} \in \mathfrak{J}_3^4, \alpha_3 \leqslant 3\} \setminus \{0\}$. Matrix $\mathbf{A}$ is an orthonormal matrix generated randomly at the beginning of our simulation.

With time step $\Delta t = 1.0 \times 10^{-3}$ and spatial grid size $\Delta x = 1/128$, the elements in the spatial basis computed by DyBO match perfectly the exact ones given by gPC as shown in Fig. 7. In Fig. 8, the $\mathbb{L}^2$ relative error of STD is plotted as a function of time t and remains very small ($\leqslant 10^{-8}$). To confirm such errors are introduced mainly by the spatial and the temporal discretizations, we use another two sets of finer grid sizes, $\Delta t = 0.5 \times 10^{-3}, \Delta x = 1/256$, and $\Delta t = 0.25 \times 10^{-3}, \Delta x = 1/512$, and repeat the computations. The STD error drops significantly since we use spectral methods and a fourth order RK method, which essentially verifies numerically Corollary 3.3.

5.3. Burgers' equation driven by stochastic forces

In the next example, we consider the stochastic Burgers equation. Stochastic Burgers equation is well known for its rich structures due to the interaction between nonlinearity and randomness and their applications in statistical mechanics, such as interfacial dynamics and directed polymers in random media and in the context of turbulence. For more discussion regarding stochastic Burgers equation and its applications, please see [6,18,27,32] and the reference therein.

Consider a one-dimensional Burgers equation driven by a zero-mean stochastic force $f(x,t,\xi(\omega))$,

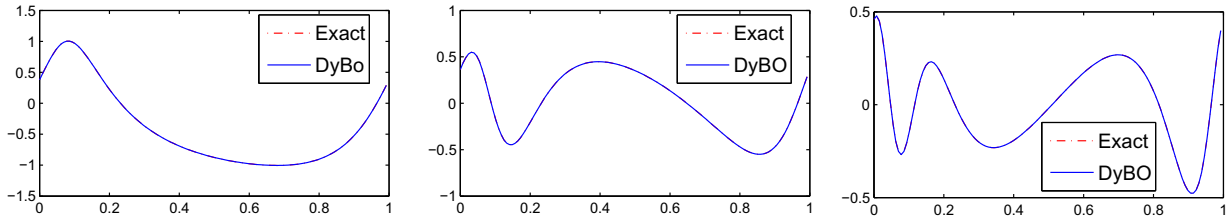

Fig. 7. The spatial basis $(u_1(x,t), u_2(x,t), u_3(x,t)$ *from the left to the right)* in the KL expansion of the SPDE solution computed by DyBO at time $t = 0.4$

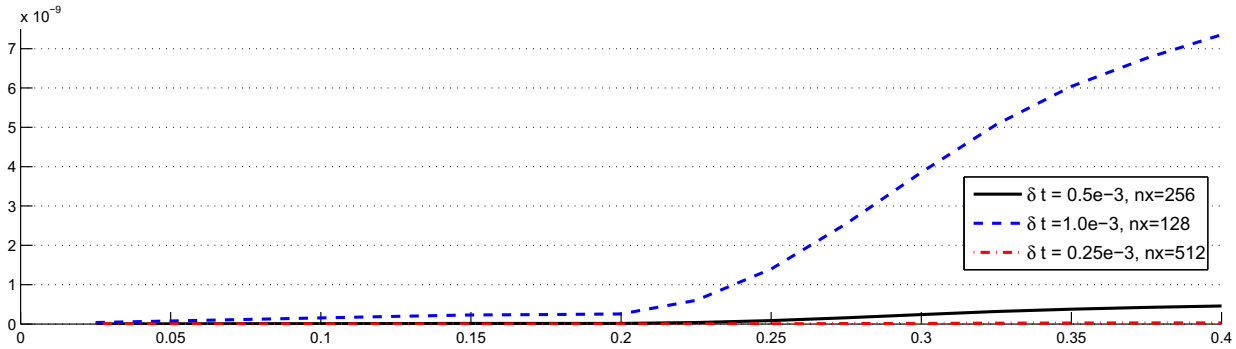

Fig. 8. $\mathbb{L}^2$ relative errors of STD computed by DyBO. The horizontal axis is time t.

$$\frac{\partial u}{\partial t} = \mathcal{L}u = \mathcal{L}\mathring{u} + f = -u\frac{\partial u}{\partial x} + \nu\frac{\partial^2 u}{\partial x^2} + f, \quad x \in [0,1], t \in [0,T], \tag{52a}$$

$$u(x,0,\xi) = u(\mathring{x}), \tag{52b}$$

$$u(0,t,\xi) = u(1,t,\xi), \tag{52c}$$

where the initial condition is deterministic and the boundary condition is periodic. Here, we call $\mathcal{L}\mathring{u} = -u\frac{\partial u}{\partial x} + \nu\frac{\partial^2 u}{\partial x^2}$ the deterministic Burgers' differential operator or Burgers' operator in short. To ensure the stochastic solution does not blow up in a finite time, we assume that $f(x,t,\xi) \in \mathbb{L}^2(\mathcal{D}\times\Omega)$ at any fixed time t and the stochastic force admits a finite-term gPC expansion, i.e., $f(x,t,\xi) = \mathbf{F}(x,t)\mathbf{H}(\xi)^T$, where the row vector $\mathbf{F} = (F_{\boldsymbol{\alpha}})_{\boldsymbol{\alpha}\in\mathfrak{J}}$ for some multi-index set $\mathfrak{J}$ with $|\mathfrak{J}| = N_p$.

When Burgers' equation is driven by stochastic processes, such as the Brownian motion, the above formulation still provides a good approximate model. The exact form of the stochastic force f can be obtained by choosing certain orthonormal basis on $\mathbb{L}^2([0,T])$ and projecting the Brownian path onto such basis. See [27,32] for details. We choose the stochastic force as $f = \sigma(x)\frac{\mathrm{d}B_t}{\mathrm{d}t}$ with $\sigma(x) = \frac{1}{2}\cos(4\pi x)$ and

$$\frac{\mathrm{d}B_t}{\mathrm{d}t} \approx \sum_{i=1}^{r}\frac{1}{\sqrt{T}}M_i\left(\frac{t}{T}\right)\xi_i = \sum_{i=1}^{r}\frac{1}{\sqrt{T}}M_i\left(\frac{t}{T}\right)\mathbf{H}_{\mathbf{e}_i} = \underbrace{\left(\frac{1}{\sqrt{T}}M_1\left(\frac{t}{T}\right), \frac{1}{\sqrt{T}}M_2\left(\frac{t}{T}\right), \cdots, \frac{1}{\sqrt{T}}M_r\left(\frac{t}{T}\right), 0, 0, \cdots, 0\right)}_{N_p \text{terms}}\mathbf{H}^T, \tag{53}$$

where $\mathbf{e}_i$ is a multi-index of length r whose ith entry is one and others are zeros, $\{M_i(t)\}_{i=1}^{\infty}$ are a complete orthonormal basis of $\mathbb{L}^2([0,1])$ and ξ_i's are i.i.d. independent standard Gaussian random variables. Further, we use the following orthonormal basis for $\mathbb{L}^2([0,T])$,

$$M_1(t) = 1, \quad M_i(t) = \sqrt{2}\cos((i-1)\pi t), \quad i = 2,3,\cdots.$$

Consider the gPC expansion of the stochastic solution $u = \bar{v} + \mathbf{V}\mathbf{H}^T$. Simple calculations give the gPC formulation for the stochastic Burgers' Eq. (52),

$$\frac{\partial \bar{v}}{\partial t} = \mathcal{L}\mathring{\bar{v}} - \mathbf{V}\frac{\partial \mathbf{V}^T}{\partial x}, \tag{54a}$$

$$\frac{\partial \mathbf{V}}{\partial t} = \left(\nu\frac{\partial^2 \mathbf{V}}{\partial x^2} - \frac{\partial(\bar{v}\mathbf{V})}{\partial x}\right) - \left(\nu_{\boldsymbol{\alpha}}\frac{\partial v_{\boldsymbol{\beta}}}{\partial x}\mathfrak{T}^{(\mathbf{H})}_{\boldsymbol{\alpha}\boldsymbol{\beta}\boldsymbol{\gamma}}\right)_{1\boldsymbol{\gamma}} + \mathbf{F}, \tag{54b}$$

where $\mathfrak{T}^{(\mathbf{H})}$ is a third-order N_p-by-N_p-by-N_p tensor, i.e., $\mathfrak{T}^{(\mathbf{H})}_{\boldsymbol{\alpha}\boldsymbol{\beta}\boldsymbol{\gamma}} = \mathbb{E}[\mathbf{H}_{\boldsymbol{\alpha}}\mathbf{H}_{\boldsymbol{\beta}}\mathbf{H}_{\boldsymbol{\gamma}}], \quad \boldsymbol{\alpha},\boldsymbol{\beta},\boldsymbol{\gamma} \in \mathfrak{J}$.

From the derivation of the gPC formulation, it is easy to see that the use of vector and tensor notations not only greatly reduces the complexity of the derivation, but also clearly reveals the structure of the gPC formulation and its relation to the deterministic Burgers' equation. For example, the mean flow $\bar{v}$ is still driven by the deterministic Burgers' differential operator $\mathcal{L}$ and exchanges energy with the stochastic flows $\mathbf{V}$ through the term $-\mathbf{V}\frac{\partial \mathbf{V}^T}{\partial x}$. The stochastic flows $\mathbf{V}$ are convected by the mean flow through term $-\frac{\partial(\bar{v}\mathbf{V})}{\partial x}$, dissipate through term $v\frac{\partial^2 \mathbf{V}}{\partial x^2}$ and interact with each others through $-(v_\alpha \frac{\partial v_\beta}{\partial x}\mathfrak{T}^{(\mathbf{H})}_{\alpha\beta\gamma})_{1\gamma}$.

Next we consider the m-term truncated KL expansion of the solution $u = \bar{u} + \mathbf{U}\mathbf{Y}^T = \bar{u} + \mathbf{U}\mathbf{A}^T\mathbf{H}^T$. The DyBO-gPC formulation of the stochastic Burgers Eq. (52) is (see Appendix B for its derivation):

$$\frac{\partial \bar{u}}{\partial t} = \mathcal{L}\mathring{\bar{u}} - \mathbf{U}\frac{\partial \mathbf{U}^T}{\partial x}, \tag{55a}$$

$$\frac{\partial \mathbf{U}}{\partial t} = -\mathbf{U}\mathbf{D}^T + \left(v\frac{\partial^2 \mathbf{U}}{\partial x^2} - \frac{\partial(\bar{u}\mathbf{U})}{\partial x}\right) - \left(u_i \frac{\partial u_j}{\partial x} A_{\alpha i}A_{\beta j}A_{\gamma k}\mathfrak{T}^{(\mathbf{H})}_{\alpha\beta\gamma}\right)_{1k} + \mathbf{F}\mathbf{A}, \tag{55b}$$

$$\frac{\mathrm{d}\mathbf{A}}{\mathrm{d}t} = \mathbf{A}\left(-\mathbf{C}^T + \left\langle v\frac{\partial^2 \mathbf{U}^T}{\partial x^2} - \frac{\partial(\bar{u}\mathbf{U}^T)}{\partial x}, \mathbf{U}\right\rangle \Lambda_{\mathbf{U}}^{-1}\right) - \left(A_{\alpha i}A_{\beta j}\mathfrak{T}^{(\mathbf{U})}_{ijk}\mathfrak{T}^{(\mathbf{H})}_{\alpha\beta\gamma}\right)_{\gamma k}\Lambda_{\mathbf{U}}^{-1} + \left\langle \mathbf{F}^T, \mathbf{U}\right\rangle \Lambda_{\mathbf{U}}^{-1}, \tag{55c}$$

where matrices $\mathbf{C}$ and $\mathbf{D}$ can be solved from the linear system (13) with

$$\Lambda_{\mathbf{U}} G_*(u, \mathbf{U}, \mathbf{Y}) = \left\langle \mathbf{U}^T, v\frac{\partial^2 \mathbf{U}}{\partial x^2} - \frac{\partial(\bar{u}\mathbf{U})}{\partial x}\right\rangle - (\mathfrak{T}^{(\mathbf{U})}_{ijl}A_{\alpha i}A_{\beta j}A_{\gamma k}\mathfrak{T}^{(\mathbf{H})}_{\alpha\beta\gamma})_{lk} + \left\langle \mathbf{U}^T, \mathbf{F}\right\rangle \mathbf{A}.$$

In the following numerical examples, the classical fourth-order RK method is used as the ODE solver and a pseudo-spectral method is applied for the spatial discretizations. We choose $r = 6$ in the stochastic force (53) and multi-index set $\mathfrak{I} = \mathfrak{I}_6^3 \setminus \{0\}$, which results in totally 83 terms in the gPC expansion, i.e., $|\mathfrak{I}| = 83$. The spatial grid size Δx is set to $1/128$ and the time step Δt is set to $0.5 \times 10^{-3}$for both gPC and DyBO, both of which are numerically integrated to time $t = T = 1.0$. 10^6 realizations are computed in the MC method to approximate the exact solution with an error of order less than 10^{-3} according to the Central Limit theorem. We choose the initial condition of the stochastic Burgers Eq. (52b) as $\mathring{u}(x) = \frac{1}{2}(e^{\cos(2\pi x)} - 1.5)\sin(2\pi(x + 0.37))$ and set the viscosity $v = 0.005$.

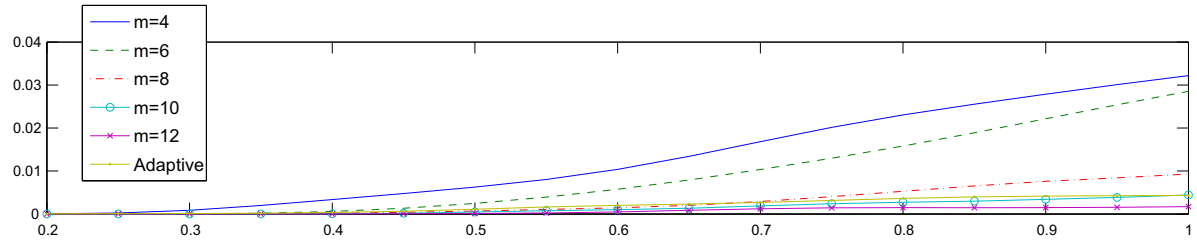

(a) Relative errors of mean

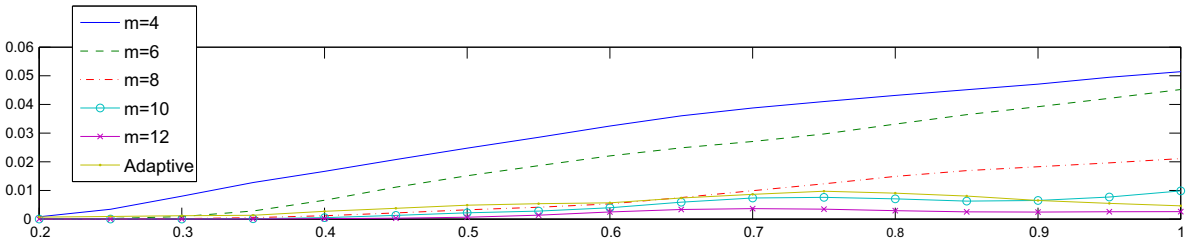

(b) Relative errors of STD

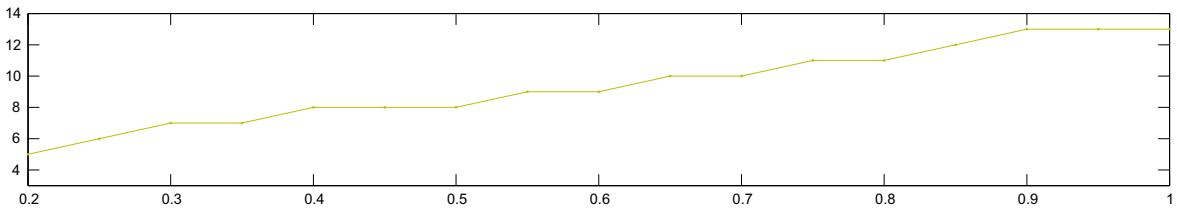

(c) Number of mode pairs

Fig. 9. $\mathbb{L}^2$ relative errors of mean and STD as functions of time.

To understand the source of errors in the DyBO method, we decompose the error into two parts. The first part of error is the difference between the DyBO solution $u^{(\mathrm{DyBO},\mathfrak{J}_r^p,m)}$ and the gPC solution $u^{(\mathrm{gPC},\mathfrak{J}_r^p)}$. The second part of error is the difference between the exact solution $u^{(\mathrm{Exact})}$ and the gPC solution, $u^{(\mathrm{gPC},\mathfrak{J}_r^p)}$. More precisely, we have

$$\epsilon = u^{(\mathrm{DyBO},\mathfrak{J}_r^p,m)} - u^{(\mathrm{Exact})} = \{u^{(\mathrm{DyBO},\mathfrak{J}_r^p,m)} - u^{(\mathrm{gPC},\mathfrak{J}_r^p)}\} + \{u^{(\mathrm{gPC},\mathfrak{J}_r^p)} - u^{(\mathrm{Exact})}\} = \epsilon_m + \epsilon_{\mathfrak{J}}.$$

The first part of the error ϵ_m diminishes as $m \to \infty$, while the second part $\epsilon_{\mathfrak{J}}$ is controlled by the multi-index set $\mathfrak{J}$ and goes to 0 as $\mathfrak{J} \to \mathfrak{J}_\infty^\infty$. Thus, there is no need to increase m any further once $\epsilon_m \ll \epsilon_{\mathfrak{J}}$. We write m^* for such m and will verify the convergence of ϵ_m and calculate m^* later.

Computational complexity of the DyBO system (55) involves considerably less work than that of the gPC system (54). Roughly speaking, for the gPC method, N_p gPC coefficients, which are functions of spatial variable x, are updated at each time iteration. However, for the DyBO method, only m spatial basis functions and one N_p-by-m matrix are updated at each time iteration. When the eigenvalues of the covariance matrix decays rapidly which is true under certain assumptions [47], m is much smaller than N_p and spatial grid number, leading to considerable computational saving.

Convergence to $u^{(\mathrm{gPC},\mathfrak{J}_r^p)}$ - Error ϵ_m. In Fig. 9, we plot the $\mathbb{L}^2$ relative errors of mean and STD computed by DyBO with $m = 4, 6, 8, 10, 12$ with respect to the gPC solution $u^{(\mathrm{gPC},\mathfrak{J}_r^p)}$. Indeed, as the number of mode pairs in DyBO increases, the $\mathbb{L}^2$ errors of mean and STD decreases, indicating the convergence of $u^{(\mathrm{DyBO},\mathfrak{J}_r^p,m)}$ to $u^{(\mathrm{gPC},\mathfrak{J}_r^p)}$. The relative errors of mean and STD at time $t = 1.0$ are also tabulated in the second and the third columns of Table 1. With $m = 12$, both errors are below 0.3%. We should point out that the DyBO-adaptive is the adaptive algorithm of DyBO method which further reduces the computational cost and improve the accuracy. The adaptive strategy will be discussed in details in the second part of our paper [11].

Direct Tracking of the KL Expansion. In Fig. 10, the first nine spatial basis at time $t = T$, i.e., $u_i(x,T), i = 1, 2, \cdots, 9$, are plotted and compared with the ones computed from $u^{(\mathrm{gPC},\mathfrak{J}_r^p)}$. Very good agreements are observed for the first six eigenfunctions (the first two rows in Fig. 10). Although the 7th, 8th and 9th spatial basis are under more influences of the unresolved mode pairs, i.e., $m+1, m+2$, etc. We still observe good agreements for these spatial basis (the last row in Fig. 10). This is because the eigenvalues corresponding to the 7th, 8th and 9th spatial basis are small.

In Fig. 11, we also plot the stochastic basis $\mathbf{Y} = \mathbf{HA}$. Since we never use directly the polynomial chaos set $\mathbf{H}$ in our computation, we plot in Fig. 11(b) the N_p-by-m matrix $\mathbf{A}$ computed in our DyBO method and in Fig. 11(c) the one computed from the gPC solution, respectively. The stochastic basis are plotted for time $t = T$. The meaning of both figures may deserve some further explanations (see Fig. 11(a)). The vertical axis from the top to the bottom is the multi-index $\boldsymbol{\alpha} \in \mathfrak{J}$, while the horizontal axis from the left to the right is the index of stochastic mode $i = 1, 2, \cdots, m$. In this setting, each column of such plot represents a single column a_j of matrix $\mathbf{A}$, i.e., a stochastic mode $Y_j = \mathbf{H}a_j$. Similarly, each row of such plot represents the projections of all stochastic basis $\mathbf{Y}$ on a certain polynomial basis $\mathbf{H}_\beta$, i.e., $\mathbb{E}[\mathbf{Y}\mathbf{H}_\beta]$. From Fig. 10 and Fig. 11, we see that the solution of DyBO can effectively track the truncated KL expansion of the stochastic Burgers' solution even if the differential operator is nonlinear.

Computational Speedup compared to gPC. Next we consider the efficiency of DyBO compared to gPC. In the fourth and fifth columns of Table 1, we also tabulate the relative errors of mean and STD computed by DyBO, with $m = 4, 6, 8, 10, 12$ and adaptive strategy, with respect to the "exact" solution $u^{(\mathrm{gPC},\mathfrak{J}_r^\infty)}$ obtained by MC method with 10^6 realizations. The relative errors of mean and STD computed by the gPC method with respect to $u^{(\mathrm{gPC},\mathfrak{J}_r^\infty)}$ are also given in the first row. Clearly, when $m = 10$ or $m = 12$, the errors of DyBO are comparable to those of gPC listed in the fist row. These results show that $\epsilon_m \ll \epsilon_{\mathfrak{J}}$ when $m = 10$ or $m = 12$, further increasing m will not decrease the overall error ϵ, i.e., $m^* = 10$ or $m^* = 12$ in this numerical example. In this case, we achieve $9.6X \sim 12.7X$ speedup.

Numerical confirmation of invariant measure. Finally we use the DyBO method to numerically confirm the invariance measure of stochastic Burgers equation. We choose $r = 8$ in the stochastic force (53) and multi-index set $\mathfrak{J} = \mathfrak{J}_8^4 \setminus \{0\}$. Sparse truncation [32] is used and results in totally 96 terms in gPC expansion, i.e., $|\mathfrak{J}| = 96$. Spatial grid size Δx is set to $1/128$ and time step Δt is set to 2.5×10^{-3} for both gPC and DyBO, both of which are numerically integrated to time $t = T = 6.0$. We choose the initial condition of the stochastic Burgers Eq. (52b) as $u(\mathring{x}) = 0.5\cos(4\pi x)$, the spatial part of the stochastic force as $\sigma(x) = 0.5\cos(2\pi x)$ and set the viscosity $\nu = 0.005$. It has been shown that the stochastic Burgers equation with Brownian forcing (52) has solutions with invariant measure if $\int_0^1 \sigma(x)dx = 0$ (see e.g. [18]). In Fig. 12, we plot the evolution history of

Table 1
Relative errors of statistical quantities computed by DyBO and gPC at time $t = 1.0$.

Methods	Compared to $u^{(\mathrm{gPC},\mathfrak{J}_r^p)}$		Compared to $u^{(\mathrm{gPC},\mathfrak{J}_r^\infty)}$		Time (min)
	Mean	STD	Mean	STD	
NA	NA	1.1619%	2.1398%	42.1	
DyBO m = 4	3.219%	5.144%	3.096%	5.556%	1.32
DyBO m = 6	2.855%	4.522%	2.935%	4.512%	2.01
DyBO m = 8	0.930%	2.112%	1.333%	2.890%	2.64
DyBO m = 10	0.444%	0.983%	1.222%	2.375%	3.32
DyBO m = 12	0.171%	0.259%	1.109%	2.122%	4.37

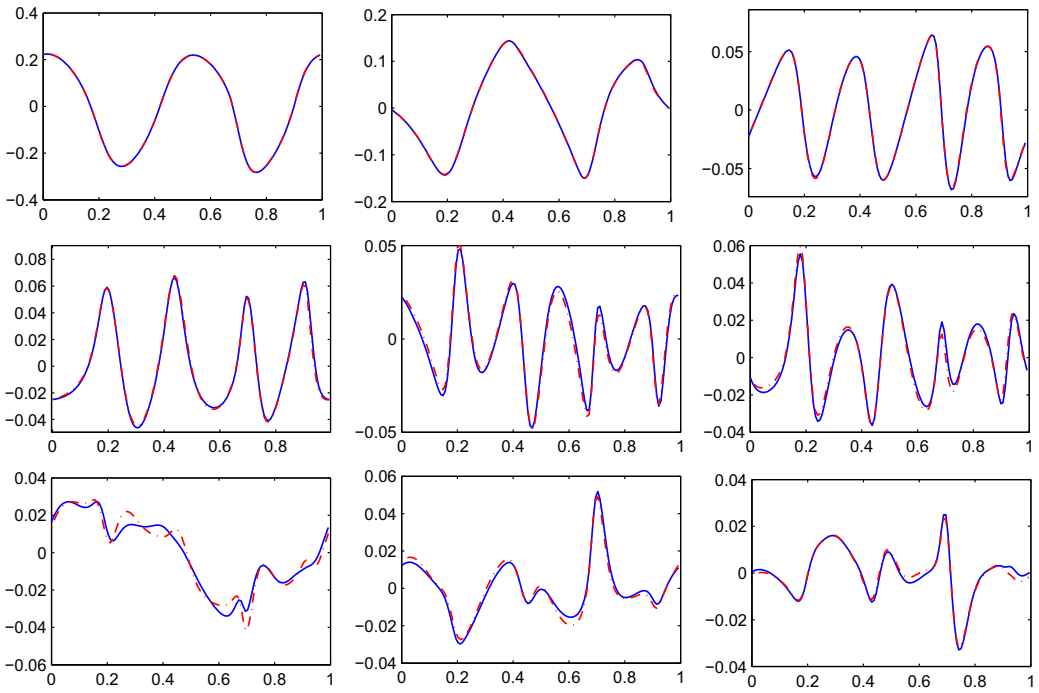

Fig. 10. The first nine spatial basis *($u_1(x,t), u_2(x,t), \cdots, u_9(x,t)$ from the left to the right and from the top to the bottom)* computed by DyBO (blue curves) at time $t = 1.0$. Red curves are given by the gPC method.(For interpretation of the references to colour in this figure caption, the reader is referred to the web version of this article.)

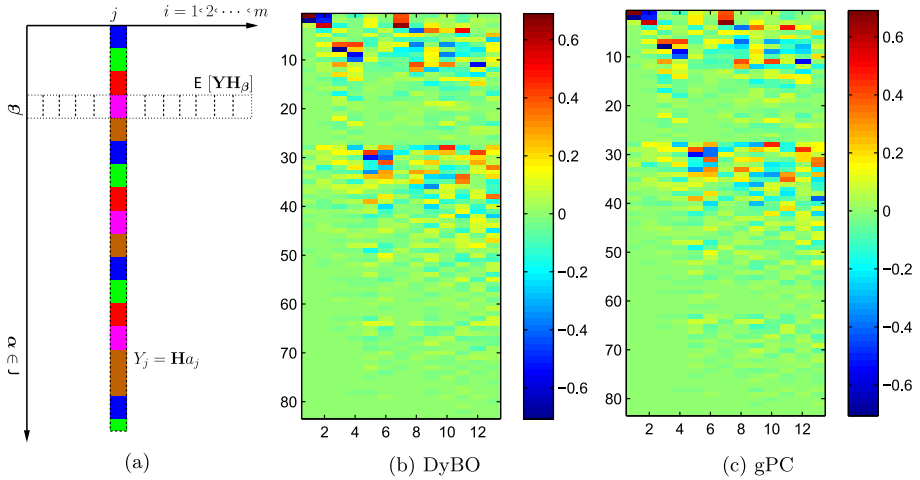

Fig. 11. Stochastic basis **HA** computed by DyBO at time $t = 1.0$.

the mean and STD of the solution. One can see that the mean and STD profiles converge to a steady state. We should point out that the adaptive DyBO method has been used in this example. Initially, we choose $m = 4$ elements in the spatial and stochastic basis, eventually we have $m = 10$. Once we reach the invariant measure, the number of modes remains the same.

6. Summary

In this paper, we have proposed and developed the DyBO method for a class of time-dependent SPDEs, whose solutions enjoy a low-dimensional structure in the sense of KL expansions. Unlike other traditional methods, such as MC, qMC, gPC, gSC, our DyBO method explores the inherent low-dimensional structure of the stochastic solution and essentially tracks the KL expansion dynamically. Thus, without the need of performing additional post-processing, the DyBO methods reveal directly the intrinsic low-dimensional structures/dynamics of related physical processes. We have proved rigorously the preservation of bi-orthogonality in DyBO methods and verified it numerically in several examples. Depending on the numerical

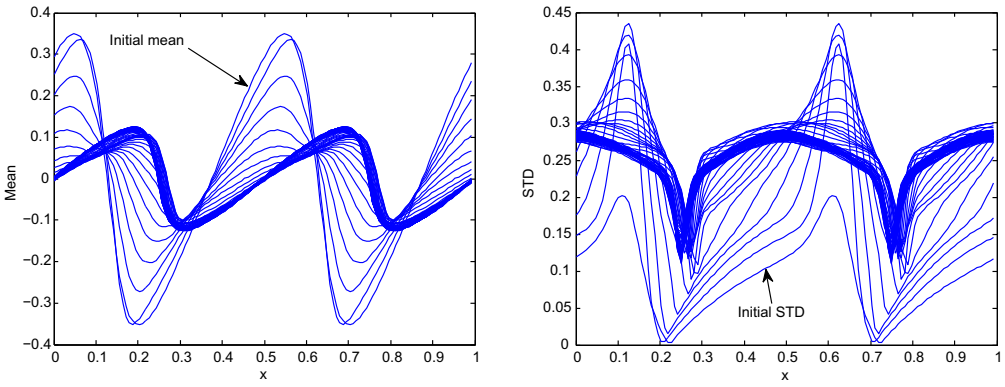

Fig. 12. Time history of the mean (left) and STD (right) of the stochastic Burgers equation for $t \leqslant 6.0$.

representations of the stochastic basis **Y**, three versions of DyBO methods have been proposed, i.e., DyBO-MC, DyBO-gSC, DyBO-gPC. We have primarily focused on DyBO-gPC in this paper. Fig. 12.

By exploring the low-dimensional structure of the solution, our DyBO methods offer considerable computational savings over other traditional methods. An important advantage of DyBO methods over other reduced basis methods is that we construct the sparsest set of spatial basis on the fly without invoking any expensive offline computations. From the perspective of gPC/gSC methods, our DyBO methods automatically use the linear combinations of polynomial chaos basis as the best set of stochastic basis on the fly without introducing any heuristics to select multi-indices.

To the best of our knowledge, the DyBO method presented in this paper is the first systematic attempt to *directly* target KL expansions and *fully* explore the bi-orthogonality. To make DyBO a feasible computational method, we have overcome several challenges in both theory and numerical implementations. From the theoretical consideration, one of the main difficulties is how to eliminate the extra degrees of freedom induced by allowing both the spatial and the stochastic basis to change in time. From numerical implementation point of view, the adoption of tensor/matrix notations enables us to present the DyBO formations in a very concise form. The vector/matrix notations also greatly simplify the codings and allow us to proceed in an intuitive way, especially for object-oriented programming languages. Temporarily freezing spatial basis **U** or stochastic basis **Y** was proposed to deal with the special moments when eigenvalues cross each other.

There are still some limitations of the DyBO method in its present form. The most important issue is how to deal with multiscale stochastic PDEs. When small scale features are important in our problem, the number of effective modes required to resolve the stochastic solution increases inversely proportional to the smallest correlation length. In this case, the effective dimension of the stochastic problem is large even if we use the KL expansion. We are currently investigating a multiscale version of the DyBO method. The main idea is to combine multiscale techniques [2,20,26] in solving deterministic PDE with the DyBO method to further reduce the computational complexity for solving multiscale SPDEs. The result will be presented in a subsequent paper. Another issue is to explore the freedom in choosing the dynamic basis to avoid the numerical difficulty associated with eigenvalue crossing. By working on an equivalent basis, we could work on a transformed space in which we can derive an evolution system without suffering from the degeneracy imposed by bi-orthogonality. By tracking this mapping dynamically, we could restore the bi-orthogonal basis on the fly. Finally, the success of our method depends critically on our ability to adaptively add or remove modes dynamically. This is one of the main topics in the second part of our paper.

Acknowledgement

This work was supported by AFOSR MURI Grant FA9550-09-1-0613, a DOE grant DE-FG02-06ER25727, and a NSF grant DMS-0908546.

Appendix A. Derivation of the DyBO formulation

In this appendix, we will complete the derivation of the DyBO formulation which we began in Section 2. We continue our derivation starting from Eq. (10). Note that Eq. (10) gives an implicit evolution system for the mean solution $\bar{u}$, the spatial basis **U** and the stochastic basis **Y** of the KL expansion. On the other hand, since $\frac{\partial \mathbf{U}}{\partial t}$ and $\frac{\mathrm{d}\mathbf{Y}}{\mathrm{d}t}$ appear on both sides of Eq. (10), we cannot use it to update the spatial basis **U** and the stochastic basis **Y**. In this subsection, we demonstrate that the partial anti-symmetrization $\tilde{\mathcal{Q}}$ of $\left\langle \mathbf{U}^T, \frac{\partial \mathbf{U}}{\partial t} \right\rangle$ in Eq. (10b) and the anti-symmetrization $\mathcal{Q}$ of $\mathbb{E}\left[\mathbf{Y}^T \frac{\mathrm{d}\mathbf{Y}}{\mathrm{d}t}\right]$ in Eq. (10c) do produce an equivalent system to the system (10) as long as **U** and **Y** are bi-orthogonal. This can be seen by taking the temporal derivative of orthogonality conditions (5a) and (5b),

$$\frac{\mathrm{d}}{\mathrm{d}t}\left\langle \mathbf{U}^T, \mathbf{U}\right\rangle = \left\langle \frac{\mathrm{d}\mathbf{U}^T}{\mathrm{d}t}, \mathbf{U}\right\rangle + \left\langle \mathbf{U}^T, \frac{\mathrm{d}\mathbf{U}}{\mathrm{d}t}\right\rangle, \tag{A.1a}$$

$$\frac{\mathrm{d}}{\mathrm{d}t}\mathbb{E}\left[\mathbf{Y}^T\mathbf{Y}\right] = \mathbb{E}\left[\frac{\mathrm{d}\mathbf{Y}^T}{\mathrm{d}t}\mathbf{Y}\right] + \mathbb{E}\left[\mathbf{Y}^T\frac{\mathrm{d}\mathbf{Y}}{\mathrm{d}t}\right]. \tag{A.1b}$$

Obviously, the off-diagonal elements of both matrices $\frac{\mathrm{d}}{\mathrm{d}t}\left\langle \mathbf{U}^T, \mathbf{U}\right\rangle$ and $\frac{\mathrm{d}}{\mathrm{d}t}\mathbb{E}\left[\mathbf{Y}^T\mathbf{Y}\right]$ are zeros due to the bi-orthogonality condition (5), which in turn implies both matrices $\left\langle \frac{\mathrm{d}\mathbf{U}^T}{\mathrm{d}t}, \mathbf{U}\right\rangle$ and $\mathbb{E}\left[\frac{\mathrm{d}\mathbf{Y}^T}{\mathrm{d}t}\mathbf{Y}\right]$ are invariant under partial anti-symmetrization $\tilde{\mathcal{Q}}$. Furthermore, $\mathbf{Y}$ being orthonormal implies $\mathbb{E}\left[\frac{\mathrm{d}\mathbf{Y}^T}{\mathrm{d}t}\mathbf{Y}\right]$ is anti-symmetric. On the other hand, bi-orthogonality (5) is preserved if it is satisfied initially at $t = 0$ and such invariance is satisfied at any later time $t > 0$. Thus, we conclude that the bi-orthogonality condition (5) is preserved for all time if and only it is true initially and the following conditions hold for any $t > 0$:

$$\tilde{\mathcal{Q}}(\left\langle \mathbf{U}^T, \frac{\partial\mathbf{U}}{\partial t}\right\rangle) = \left\langle \mathbf{U}^T, \frac{\partial\mathbf{U}}{\partial t}\right\rangle, \tag{A.2a}$$

$$\mathcal{Q}(\mathbb{E}\left[\mathbf{Y}^T\frac{\mathrm{d}\mathbf{Y}}{\mathrm{d}t}\right]) = \mathbb{E}\left[\mathbf{Y}^T\frac{\mathrm{d}\mathbf{Y}}{\mathrm{d}t}\right]. \tag{A.2b}$$

In other words, anti-symmetrization enforces the bi-orthogonality condition, which essentially characterizes KL expansions. After applying this result to the system (10), we arrive at

$$\frac{\partial\bar{u}}{\partial t} = \mathbb{E}[\mathcal{L}\tilde{u}], \tag{A.3a}$$

$$\frac{\partial\mathbf{U}}{\partial t} = \mathbf{U}\mathbf{\Lambda}_{\mathbf{U}}^{-1}\tilde{\mathcal{Q}}\left(\left\langle \mathbf{U}^T, \frac{\partial\mathbf{U}}{\partial t}\right\rangle\right) + G_{\mathbf{U}}(\bar{u}, \mathbf{U}, \mathbf{Y}), \tag{A.3b}$$

$$\frac{\mathrm{d}\mathbf{Y}}{\mathrm{d}t} = \mathbf{Y}\mathcal{Q}\left(\mathbb{E}\left[\mathbf{Y}^T\frac{\mathrm{d}\mathbf{Y}}{\mathrm{d}t}\right]\right) + G_{\mathbf{Y}}(\bar{u}, \mathbf{U}, \mathbf{Y}). \tag{A.3c}$$

Next, we will eliminate the time derivatives from the right hand sides in Eq. (A.3b) and Eq. (A.3c). We first observe that Eq. (A.3b) does not determine $\frac{\partial\mathbf{U}}{\partial t}$ uniquely. In fact, $\frac{\partial\mathbf{U}}{\partial t} - \mathbf{U}\mathbf{\Lambda}_{\mathbf{U}}^{-1}\tilde{\mathcal{Q}}(\left\langle \mathbf{U}^T, \frac{\partial\mathbf{U}}{\partial t}\right\rangle)$ is the projection of $\frac{\partial\mathbf{U}}{\partial t}$ into the orthogonal complementary set of $\mathbf{U}$. Thus, we cannot determine the projection of $\frac{\partial\mathbf{U}}{\partial t}$ into the space spanned by $\mathbf{U}$ from Eq. (A.3b). Notice that $(\mathbf{U}, \tilde{\mathbf{U}})$ forms a complete orthogonal basis in the physical space for any given time. To determine the projection of $\frac{\partial\mathbf{U}}{\partial t}$ in the space spanned by $\mathbf{U}$, we express $\frac{\partial\mathbf{U}}{\partial t}$ in terms of the complete orthogonal basis given by $(\mathbf{U}, \tilde{\mathbf{U}})$:

$$\frac{\partial\mathbf{U}}{\partial t} = \mathbf{U}\mathbf{C} + \tilde{\mathbf{U}}\tilde{\mathbf{C}}, \tag{A.4}$$

where $\mathbf{C}(t) \in \mathbb{R}^{m\times m}$ and $\tilde{\mathbf{C}}(t) \in \mathbb{R}^{\infty\times m}$. We will show that $\tilde{\mathbf{U}}\tilde{\mathbf{C}} = G_{\mathbf{U}}(\bar{u}, \mathbf{U}, \mathbf{Y})$. We note that $\mathbf{U}\mathbf{C}$ is the projection of $\frac{\partial\mathbf{U}}{\partial t}$ into $\mathbf{U}$. The matrix $\mathbf{C}$ represents the extra degrees of freedom in evolving $\frac{\partial\mathbf{U}}{\partial t}$. We will determine these extra degrees of freedom by enforcing the bi-orthogonal condition and a compatibility condition. Note that

$$\left\langle \mathbf{U}^T, \frac{\partial\mathbf{U}}{\partial t}\right\rangle = \left\langle \mathbf{U}^T, \mathbf{U}\mathbf{C} + \tilde{\mathbf{U}}\tilde{\mathbf{C}}\right\rangle = \left\langle \mathbf{U}^T, \mathbf{U}\right\rangle\mathbf{C} + \left\langle \mathbf{U}^T, \tilde{\mathbf{U}}\right\rangle\tilde{\mathbf{C}} = \left\langle \mathbf{U}^T, \mathbf{U}\right\rangle\mathbf{C}. \tag{A.5}$$

Substituting Eq. (A.5) and Eq. (A.4) into Eq. (A.3b) gives

$$\mathbf{U}(\mathbf{C} - \mathbf{\Lambda}_{\mathbf{U}}^{-1}\tilde{\mathcal{Q}}(\mathbf{\Lambda}_{\mathbf{U}}\mathbf{C})) = G_{\mathbf{U}}(\bar{u}, \mathbf{U}, \mathbf{Y}) - \tilde{\mathbf{U}}\tilde{\mathbf{C}}. \tag{A.6}$$

Recall that the left side of Eq. (A.6) is in $\mathrm{span}(\mathbf{U}) \subset \mathbb{L}^2(\mathcal{D})$ while the right side is in its orthogonal complement. We obtain

$$\mathbf{C} - \mathbf{\Lambda}_{\mathbf{U}}^{-1}\tilde{\mathcal{Q}}(\mathbf{\Lambda}_{\mathbf{U}}\mathbf{C}) = 0, \tag{A.7a}$$

$$\tilde{\mathbf{U}}\tilde{\mathbf{C}} = G_{\mathbf{U}}(\bar{u}, \mathbf{U}, \mathbf{Y}). \tag{A.7b}$$

Similarly, the change of the stochastic basis, $\frac{\mathrm{d}\mathbf{Y}}{\mathrm{d}t}$, can be written in the form of

$$\frac{\mathrm{d}\mathbf{Y}}{\mathrm{d}t} = \mathbf{Y}\mathbf{D} + \tilde{\mathbf{Y}}\tilde{\mathbf{D}}, \tag{A.8}$$

where $\mathbf{D}(t) \in \mathbb{R}^{m\times m}$ and $\tilde{\mathbf{D}}(t) \in \mathbb{R}^{\infty\times m}$. We will show that $\tilde{\mathbf{Y}}\tilde{\mathbf{D}} = G_{\mathbf{Y}}(\bar{u}, \mathbf{U}, \mathbf{Y})$. We note that $\mathbf{Y}\mathbf{D}$ is the projection of $\frac{\mathrm{d}\mathbf{Y}}{\mathrm{d}t}$ into the space spanned by $\mathbf{Y}$. The matrix $\mathbf{D}$ represents the extra degrees of freedom in evolving $\frac{\mathrm{d}\mathbf{Y}}{\mathrm{d}t}$. First, we observe that

$$\mathbb{E}\left[\mathbf{Y}^T\frac{\mathrm{d}\mathbf{Y}}{\mathrm{d}t}\right] = \mathbb{E}[\mathbf{Y}]^T\mathbf{Y}\mathbf{D} + \mathbb{E}\left[\mathbf{Y}^T\tilde{\mathbf{Y}}\right]\tilde{\mathbf{D}} = \mathbf{D}. \tag{A.9}$$

Substituting Eq. (A.9) and Eq. (A.8) into Eq. (A.3c), we get

$$\mathbf{Y}(\mathbf{D}-\mathcal{Q}(\mathbf{D}))=G_{\mathbf{Y}}(\bar{u},\mathbf{U},\mathbf{Y})-\tilde{\mathbf{Y}}\tilde{\mathbf{D}}. \tag{A.10}$$

Note that the left side of Eq. (A.10) is in $\mathrm{span}(\mathbf{Y})\subset\mathbb{L}^2(\Omega)$ and the right side is in its orthogonal complement. This gives rise to the following equations:

$$\mathbf{D}-\mathcal{Q}(\mathbf{D})=0, \tag{A.11a}$$

$$\tilde{\mathbf{Y}}\tilde{\mathbf{D}}=G_{\mathbf{Y}}(\bar{u},\mathbf{U},\mathbf{Y}). \tag{A.11b}$$

However, Eq. (A.7a) and Eq. (A.11a) are not sufficient to determine matrices $\mathbf{C}$ and $\mathbf{D}$. To find additional equations for $\mathbf{C}$ and $\mathbf{D}$, we substitute Eq. (A.4) and Eq. (A.8) back into the original stochastic partial differential Eq. (1a) and get

$$\mathbf{U}(\mathbf{D}^T+\mathbf{C})\mathbf{Y}^T+\mathbf{U}\tilde{\mathbf{D}}^T\tilde{\mathbf{Y}}^T+\tilde{\mathbf{U}}\tilde{\mathbf{C}}\mathbf{Y}^T=\tilde{\mathcal{L}}\tilde{u}. \tag{A.12}$$

Multiplying $\mathbf{U}^T$ from the left and $\mathbf{Y}$ from the right on both sides of Eq. (A.12) and taking inner products $\langle\cdot,\cdot\rangle$ and expectations $\mathbb{E}[\cdot]$, we obtain the following compatibility condition for C and D:

$$\mathbf{D}^T+\mathbf{C}=G_*(\bar{u},\mathbf{U},\mathbf{Y}), \tag{A.13}$$

where we have used (5a), (5b) and $G_*(\bar{u},\mathbf{U},\mathbf{Y})=\mathbf{\Lambda}_{\mathbf{U}}^{-1}\left\langle\mathbf{U}^T,\mathbb{E}\left[\tilde{\mathcal{L}}\tilde{u}\mathbf{Y}\right]\right\rangle\in\mathbb{R}^{m\times m}$. Using Eq. (A.7a), Eq. (A.11a), and the compatibility condition (A.13), we can determine $\mathbf{C}$ and $\mathbf{D}$ uniquely provided that $\langle u_i,u_i\rangle\neq\langle u_j,u_j\rangle$ for $i\neq j$. This completes our derivation of the DyBO formulation.

Appendix B. Derivation of the DyBO-gPC formulation of stochastic burgers equation

In this appendix, we provide a detailed derivation of Eq. (52). Consider the m-term truncated KL expansion of the stochastic Burgers equation solution $\tilde{u}=\bar{u}+\mathbf{U}\mathbf{Y}^T=\bar{u}+\mathbf{U}\mathbf{A}^T\mathbf{H}^T$. Simple calculations give

$$\mathcal{L}\tilde{u}=-\left(\bar{u}+\mathbf{U}\mathbf{Y}^T\right)\left(\frac{\partial\bar{u}}{\partial x}+\frac{\partial\mathbf{U}}{\partial x}\mathbf{Y}^T\right)+\nu\left(\frac{\partial^2\bar{u}}{\partial x^2}+\frac{\partial^2\mathbf{U}}{\partial x^2}\mathbf{Y}^T\right)+f=\mathring{\mathcal{L}}\bar{u}+\left(\nu\frac{\partial^2\mathbf{U}}{\partial x^2}-\frac{\partial(\bar{u}\mathbf{U})}{\partial x}\right)\mathbf{Y}^T-\mathbf{U}\mathbf{Y}^T\mathbf{Y}\frac{\partial\mathbf{U}^T}{\partial x}+f.$$

Thus, we have

$$\mathbb{E}[\mathcal{L}\tilde{u}]=\mathring{\mathcal{L}}\bar{u}-\mathbf{U}\frac{\partial\mathbf{U}^T}{\partial x},$$

where we have used $\mathbb{E}\left[\mathbf{Y}^T\mathbf{Y}\right]=\mathbf{I}$, $\mathbb{E}[\mathbf{Y}]=0$, and $\mathbb{E}[f]=0$. Direct calculations give

$$\tilde{\mathcal{L}}\tilde{u}=\left(\nu\frac{\partial^2\mathbf{U}}{\partial x^2}-\frac{\partial(\bar{u}\mathbf{U})}{\partial x}\right)\mathbf{Y}^T-\mathbf{U}\mathbf{Y}^T\mathbf{Y}\frac{\partial\mathbf{U}^T}{\partial x}+\mathbf{U}\frac{\partial\mathbf{U}^T}{\partial x}+f,\mathbb{E}\left[\tilde{\mathcal{L}}\tilde{u}\mathbf{Y}\right]=\left(\nu\frac{\partial^2\mathbf{U}}{\partial x^2}-\frac{\partial(\bar{u}\mathbf{U})}{\partial x}\right)+\mathbb{E}[f\mathbf{Y}]-\mathbb{E}\left[\mathbf{U}\mathbf{Y}^T\mathbf{Y}\frac{\partial\mathbf{U}^T}{\partial x}\mathbf{Y}\right],$$

$$\left\langle\tilde{\mathcal{L}}\tilde{u},\mathbf{U}\right\rangle=\mathbf{Y}\left\langle\nu\frac{\partial^2\mathbf{U}^T}{\partial x^2}-\frac{\partial(\bar{u}\mathbf{U}^T)}{\partial x},\mathbf{U}\right\rangle+\langle f,\mathbf{U}\rangle+\left\langle\mathbf{U}\frac{\partial\mathbf{U}^T}{\partial x},\mathbf{U}\right\rangle-\left\langle\mathbf{U}\mathbf{Y}^T\mathbf{Y}\frac{\partial\mathbf{U}^T}{\partial x},\mathbf{U}\right\rangle,$$

$$\mathbf{\Lambda}_{\mathbf{U}}G_*(\bar{u},\mathbf{U},\mathbf{Y})=\left\langle\mathbf{U}^T,\nu\frac{\partial^2\mathbf{U}}{\partial x^2}-\frac{\partial(\bar{u}\mathbf{U})}{\partial x}\right\rangle+\left\langle\mathbf{U}^T,\mathbb{E}[f\mathbf{Y}]\right\rangle-\left\langle\mathbf{U}^T,\mathbb{E}\left[\mathbf{U}\mathbf{Y}^T\mathbf{Y}\frac{\partial\mathbf{U}^T}{\partial x}\mathbf{Y}\right]\right\rangle,$$

where the last terms on the right hand sides of the last three equations can be written in component forms, for $i,j,k=1,2,\cdots,m$,

$$\mathbb{E}\left[\mathbf{U}\mathbf{Y}^T\mathbf{Y}\frac{\partial\mathbf{U}^T}{\partial x}\mathbf{Y}\right]=\left(\mathbb{E}\left[u_iY_iY_j\frac{\partial u_j}{\partial x}Y_k\right]\right)_{1k}=\left(u_i\frac{\partial u_j}{\partial x}\mathbb{E}\left[Y_iY_jY_k\right]\right)_{1k},\left\langle\mathbf{U}\mathbf{Y}^T\mathbf{Y}\frac{\partial\mathbf{U}^T}{\partial x},\mathbf{U}\right\rangle=\left(\left\langle u_iY_iY_j\frac{\partial u_j}{\partial x},u_k\right\rangle\right)_{1k}$$

$$=\left(Y_iY_j\left\langle u_i\frac{\partial u_j}{\partial x},u_k\right\rangle\right)_{1k},\left\langle\mathbf{U}^T,\mathbb{E}\left[\mathbf{U}\mathbf{Y}^T\mathbf{Y}\frac{\partial\mathbf{U}^T}{\partial x}\mathbf{Y}\right]\right\rangle=\left(\left\langle u_i\frac{\partial u_j}{\partial x},u_l\right\rangle\mathbb{E}\left[Y_iY_jY_k\right]\right)_{lk},$$

where $(\cdot)_{1k}$ and $(\cdot)_{lk}$ emphasize row vector and m-by-m matrix, respectively. We write third-order m-by-m-by-m tensors

$$\mathfrak{T}^{(\mathbf{Y})}_{ijk}=\mathbb{E}\left[Y_iY_jY_k\right]\quad\text{and}\quad\mathfrak{T}^{(\mathbf{U})}_{ijl}=\left\langle u_i\frac{\partial u_j}{\partial x},u_l\right\rangle\quad i,j,k,l=1,2,\cdots,m.$$

Clearly, $\mathfrak{T}^{(\mathbf{Y})}$ is symmetric with respect to all three indices, i.e., $\mathfrak{T}^{(\mathbf{Y})}_{ijk}=\mathfrak{T}^{(\mathbf{Y})}_{\mathrm{perm}(ijk)}$ for $\forall i,j,k\in\{1,2,\cdots,m\}$, where $\mathrm{perm}(ijk)$ is any permutation of indices i,j,k, and $\mathfrak{T}^{(\mathbf{U})}$ is symmetric with respect to the first and the third indices, i.e., $\mathfrak{T}^{(\mathbf{U})}_{ijk}=\mathfrak{T}^{(\mathbf{U})}_{kji}$ for $\forall i,k\in\{1,2,\cdots,m\}$. Such symmetries can be explored in numerical implementations to achieve further computational reductions. Using Eq. (15), we obtain the DyBO formulation,

$$\frac{\partial \bar{u}}{\partial t} = \mathring{\mathcal{L}}\bar{u} - \mathbf{U}\frac{\partial \mathbf{U}^T}{\partial x}, \tag{B.1a}$$

$$\frac{\partial \mathbf{U}}{\partial t} = -\mathbf{U}\mathbf{D}^T + \left(\nu\frac{\partial^2 \mathbf{U}}{\partial x^2} - \frac{\partial(\bar{u}\mathbf{U})}{\partial x}\right) - \left(u_i\frac{\partial u_j}{\partial x}\mathfrak{T}^{(\mathbf{Y})}_{ijk}\right)_{1k} + \mathbb{E}[f\mathbf{Y}], \tag{B.1b}$$

$$\frac{\mathrm{d}\mathbf{Y}}{\mathrm{d}t} = \mathbf{Y}\left(-\mathbf{C}^T + \left\langle \nu\frac{\partial^2 \mathbf{U}^T}{\partial x^2} - \frac{\partial(\bar{u}\mathbf{U}^T)}{\partial x}, \mathbf{U}\right\rangle \mathbf{\Lambda}_{\mathbf{U}}^{-1}\right) + \left(\mathfrak{T}^{(\mathbf{U})}_{iik}\right)_{1k}\mathbf{\Lambda}_{\mathbf{U}}^{-1} \tag{B.1c}$$

where

$$\mathbf{\Lambda}_{\mathbf{U}}G_*(\bar{u},\mathbf{U},\mathbf{Y}) = \left\langle \mathbf{U}^T, \nu\frac{\partial^2 \mathbf{U}}{\partial x^2} - \frac{\partial(\bar{u}\mathbf{U})}{\partial x}\right\rangle - \left(\mathfrak{T}^{(\mathbf{U})}_{ijl}\mathfrak{T}^{(\mathbf{Y})}_{ijk}\right)_{lk} + \left\langle \mathbf{U}^T, \mathbb{E}[f\mathbf{Y}]\right\rangle. \tag{B.2}$$

Similarly, the DyBO-gPC formulation can be obtained by substituting $\mathbf{Y} = \mathbf{H}\mathbf{A}$ into (B.1a)(B.2) and using the face $\mathbb{E}\left[\mathbf{Y}^T\mathbf{Y}\right] = \mathbf{A}^T\mathbf{A} = \mathbf{I}$.

References

[1] I. Babuska, F. Nobile, R. Tempone, A stochastic collocation method for elliptic partial differential equations with random input data, SIAM J. Numer. Anal. 45 (3) (2007) 1005.
[2] A. Bensoussan, J.-L. Lions, G. Papanicolaou, Asymptotic Analysis for Periodic Structure, North-Holland, Amsterdam, 1978.
[3] G. Berkooz, P. Holmes, J.L. Lumley, The proper orthogonal decomposition in the analysis of turbulent flows, Ann. Rev. Fluid Mech. 25 (1993) 539–575.
[4] L. Borcea, G. Papanicolaou, C. Tsogka, J. Berryman, Imaging and time reversal in random media, Inverse Prob. 18 (2002) 1247–1279.
[5] L. Borcea, G. Papanicolaou, C. Tsogka, Theory and applications of time reversal and interferometric imaging, Inverse Prob. 19 (2002) 139–164.
[6] J.P. Bouchaud, M. Mezard, G. Parisi, Scaling and intermittency in Burgers turbulence, Phys. Rev. E1 52 (4) (1995) 3656–3674.
[7] S. Boyaval, C. LeBris, T. Lelièvre, Y. Maday, N. Nguyen, A. Patera, Reduced basis techniques for stochastic problems, Arch. Comput. Meth. Eng. 17 (2012) 435–454.
[8] H.J. Bungartz, M. Griebel, Sparse grids, Acta Numer. 13 (2004) 147–269.
[9] R.H. Cameron, W.T. Martin, The orthogonal developement of non-linear functionals in series of fourier-hermite functionals, Ann. Math. 48 (2) (1947) 385–392.
[10] M.L. Cheng, Adaptive methods exploring intrinsic sparse structures of stochastic partial differential equations, Doctroal thesis California Institute of Technology, 2012.
[11] M.L. Cheng, T.Y. Hou, Z.W. Zhang, A dynamically bi-orthogonal method for time-dependent stochastic partial differential equations II: adaptivity and generalizations, J. Comput. Phys. Accepted for publication, http://dx.doi.org/10.1016/j.jcp.2013.02.020.
[12] A.J. Chorin, Hermite expansion in Monte-Carlo simulations, J. Comput. Phys. 8 (1971) 472–482.
[13] A.J. Chorin, Gaussian fields and random flow, J. Fluid Mech. 63 (1974) 21–32.
[14] A.J. Chorin, X.M. Tu, Implicit sampling for particle filters, Proc. Nat. Acad. Sci. 106 (2009) 17249–17254.
[15] M. Dashti, A.M. Stuart, Uncertainty quantification and weak approximation of an elliptic inverse problem, SIAM J. Numer. Anal. 49 (2011) 2524–2542.
[16] A. Doostan, H. Owhadi, A non-adapted sparse approximation of PDEs with stochastic inputs, J. Comput. Phys. 230 (8) (2011) 3015–3034.
[17] P. Dostert, Y. Efendiev, T.Y. Hou, W. Luo, Coarse gradient Langevin algorithms for dynamic data integration and uncertainty quantification, J. Comput. Phys. 217 (2006) 123–142.
[18] W. E, K. Khanin, A. Mazel, Y. Sinai, Invariant measures for Burgers equation with stochastic forcing, Ann. Math. 151 (3) (2000) 877–960.
[19] Y. Efendiev, T.Y. Hou, W. Luo, Preconditioning of Markov Chain Monte Carlo simulations using coarse-scale models, SIAM J. Sci. Comput. 28 (2) (2006) 776–803.
[20] Y. Efendiev, T.Y. Hou, Multiscale Finite Element Methods: Theory and Applications, Springer, New York, 2009.
[21] Y. Efendiev, J. Galvis, T.Y. Hou, Generalized Multiscale Finite Element Methods (GMsFEM), J. Comput. Phys., submitted for publication.
[22] J.N. Franklin, Matrix Theory, Dover Books on Mathematics, First ed., Dover Publications, 2000.
[23] R.G. Ghanem, P.D. Spanos, Stochastic Finite Elements: A Spectral Approach, Springer-Verlag, New York, 1991.
[24] M.B. Giles, Multilevel Monte Carlo path simulation, Oper. Res. 56 (3) (2008) 607–617.
[25] I. Hosokawa, K. Yamamoto, Turbulence in randomly force, one-dimensional Burgers flow, J. Stat. Phys. 13 (3) (1975) 245–272.
[26] T.Y. Hou, X.H. Wu, A multiscale finite element method for elliptic problems in composite materials and porous media, J. Comput. Phys. 134 (1997) 169–189.
[27] T.Y. Hou, W. Luo, B. Rozovskii, H. Zhou, Wiener Chaos expansions and numerical solutions of randomly forced equations of fluid mechanics, J. Comput. Phys. 216 (2) (2006) 687–706.
[28] K. Karhunen, Uber lineare Methoden in der Wahrscheinlichkeitsrechnung, Ann. Acad. Sci. Fennicae. Ser. A.I. Math.-Phys. 37 (1947) 1–79.
[29] P.E. Kloeden, E. Platen, Numerical Solution of Stochastic Differential Equations, Springer-Verlag Berlin, Heidelberg, 1992.
[30] L.Y. Li, H.A. Tchelepi, D.X. Zhang, Perturbation-based moment equation approach for flow in heterogeneous porous media: applicability range and analysis of high-order terms, J. Comput. Phys. 188 (1) (2003) 296–317.
[31] M. Loeve, Probability Theory. Vol. II, 4th ed. GTM. 46. Springer-Verlag. ISBN 0-387-90262-7.
[32] W. Luo, Wiener chaos expansion and numerical solutions of stochastic partial differential equations, Ph.D. thesis, California Institute of Technology, 2006.
[33] X. Ma, N. Zabaras, An adaptive hierarchical sparse grid collocation algorithm for the solution of stochastic differential equations, J. Comput. Phys. 228 (8) (2009) 3084–3113.
[34] Y. Maday, Reduced-basis method for the rapid and reliable solution of partial differential equations, Proceedings of international conference of mathematicians, European Mathematical Society, Madrid, Zurich, 2006.
[35] O. Le Maitre, Uncertainty propagation using Wiener–Haar expansions, J. Comput. Phys. 197 (1) (2004) 28–57.
[36] O. Le Maitre, A Newton method for the resolution of steady stochastic Navier–Stokes equations, Comput. Fluids 38 (8) (2009) 1566–1579.
[37] A.J. Majda, I. Timofeyev, E.V. Eijnden, A mathematical framework for stochastic climate models, CPAM 54 (2001) 891–974.
[38] A.J. Majda, C. Franzke, B. Khouider, An applied mathematics perspective on stochastic modeling for climate, Philos. Trans. R. Soc. 366 (2008) 2427–2453.
[39] A.J. Majda, M. Branicki, Lessons in Uncertainty Quantification for Turbulent Dynamical System, DCDS-A 32 (2012) 3133–3221.
[40] W.J. Morokoff, R.E. Caflisch, Quasi-random sequences and their discrepancies, SIAM J. Sci. Comput. 15 (6) (1994) 1251–1279.
[41] H.N. Najm, Uncertainty quantification and polynomial chaos techniques in computational fluid dynamics, Ann. Rev. Fluid Mech. 41 (1) (2009) 35–52.
[42] H. Niederreiter, Random number generation and Quasi–Monte Carlo methods, SIAM Publ., 1992.

[43] H. Owhadi, C. Scovel, T.J. Sullivan, M. McKerns, M. Ortiz. Optimal uncertainty quantification, SIAM Review, in press, arXiv:1009.0679.
[44] G. Rozza, D.B.P. Huynh, A.T. Patera, Reduced basis approximation and a posteriori error estimation for affinely parametrized elliptic coercive partial differential equations Application to transport and continuum mechanics, Arch. Comput. Meth. Eng. (3) (2008) 229–275.
[45] T.P. Sapsis, P.F.J. Lermusiaux, Dynamically orthogonal field equations for continuous stochastic dynamical systems, Physica D 238 (2009) 2347–2360.
[46] T.P. Sapsis, P.F.J. Lermusiaux, Dynamical criteria for the evolution of the stochastic dimensionality in flows with uncertainty, Physica D 241 (1) (2012) 60–76.
[47] C. Schwab, R.A. Todor, Karhunen–Loeve approximation of random fields by generalized fast multipole methods, J. Comput. Phys. 217 (2006) 100–122.
[48] D. Venturi, On proper orthogonal decomposition of randomly perturbed fields with applications to flow past a cylinder and natural convection over a horizontal plate, J. Fluid Mech. 559 (2006) 215–254.
[49] D. Venturi, X. Wan, G.E. Karniadakis, Stochastic low-dimensional modeling of a random laminar wake past a circular cylinder, J. Fluid Mech. 606 (2008) 339–367.
[50] X. Wan, G.E. Karniadakis, An adaptive multi-element generalized polynomial chaos method for stochastic differential equations, J. Comput. Phys. 209 (2) (2005) 617–642.
[51] N. Wierner, The homogeneous chaos, Am. J. Math. 60 (1938) 897–936.
[52] X.-H. Wu, L. Bi, S. Kalla, Effective parametrization for reliable reservoir performance predictions, Int. J. Uncertainty Quantification 2 (3) (2012) 259–278.
[53] D. Xiu, G.E. Karniadakis, The Wiener–Askey polynomial chaos for stochastic differential equations, SIAM J. Sci. Comput. 24 (2) (2002) 614–644.
[54] D. Xiu, G.E. Karniadakis, Modeling uncertainty in flow simulations via generalized polynomial chaos, J. Comput. Phys. 187 (1) (2003) 137–167.